Universidade de Aveiro Departamento de Ciências Médicas
2017

MARIANA CAMPOS MARQUES

Respostas Celulares à Infeção Viral: Proteostase e Imunidade Inata

Cellular Responses to Viral Infection: Proteostasis And Innate Immunity

Universidade de Aveiro Departamento de Ciências Médicas
2017

MARIANA CAMPOS MARQUES

Respostas Celulares à Infeção Viral: Proteostase e Imunidade Inata

Cellular Responses to Viral Infection: Proteostasis And Innate Immunity

Tese apresentada à Universidade de Aveiro para cumprimento dos requisitos necessários à obtenção do grau de Mestre em Biomedicina Molecular, realizada sob a orientação científica da Doutora Daniela Maria Oliveira Gandra Ribeiro, Professora Auxiliar Convidada do Departamento de Ciências Médicas da Universidade de Aveiro e Investigadora Principal do grupo “Organelle Dynamics in Infection and Disease” do Instituto de Investigação em Biomedicina (iBiMED), Universidade de Aveiro.

Thesis submitted at University of Aveiro to fulfil the requirements to obtain the Master degree in Molecular Biomedicine, held under the scientific guidance of Dr. Daniela Maria Oliveira Gandra Ribeiro, Principal Investigator at Organelle Dynamics in Infection and Disease group at Institute for Research in Biomedicine (iBiMED), University of Aveiro.

o júri

presidente	Doutora Ana Gabriela Henriques Professora Auxiliar Convidada do Departamento de Ciências Médicas da Universidade de Aveiro
	Doutora Daniela Maria Oliveira Gandra Ribeiro Professora Auxiliar Convidada do Departamento de Ciências Médicas da Universidade de Aveiro
	Doutora Rute Conceição do Nascimento Veríssimo Afonso Bolseira de pós-doutoramento do Instituto Gulbenkian de Ciência e Médica Interna de Ano Comum do CHO- Centro Hospitalar Oeste

agradecimentos

Um grande obrigado a todos os que me acompanharam ao longo desta etapa e que, de uma maneira ou de outra, me ajudaram a chegar ao fim.

À Dra. Daniela Ribeiro, por me ter apoiado a dar os primeiros passos na investigação, por ter orientado o desenvolver deste projeto, por toda a experiência que me transmitiu, por todos os conselhos, e por me contagiar com o seu entusiasmo pelo mundo da virologia.

A todos os que partilharam e têm vindo a partilhar comigo a experiência de trabalhar no ODID Lab, especialmente por me terem integrado tão bem dentro e fora laboratório. Foi e tem sido um prazer fazer parte deste grupo.
À Isabel, obrigada por toda a ajuda, por partilhares os teus conhecimentos comigo, pela companhia e por enriqueceres o meu vocabulário com as tuas expressões malucas.
À Beatriz, por estares sempre pronta a ajudar-me e por animares os meus dias de trabalho sempre com uma banda sonora.
À Joana, ao Ricardo, à Catarina e ao Rui pela companhia e por partilharem comigo o que é iniciar um projeto num grupo novo.
Um especial e enorme agradecimento à Rita, por todas as horas boas e menos boas. Por acreditar em mim e no meu trabalho, por tudo o que me ensinaste e por me ajudares a ultrapassar os mil e um problemas que foram surgindo, mesmo com um oceano pelo meio. Por teres partilhado comigo alguns segredos de Aveiro, pelos passeios e pelos petiscos, sobretudo pela tua amizade.

À Carolina e à Marisa por me terem aturado mais do que deviam, sempre prontas a aliviar os ânimos. Por toda a vossa ajuda no decorrer das experiências, a analisar os resultados e a encontrar soluções.

À Dra. Ana Soares, por me ter ajudado em todas das situações em que me ajudou a perceber "o que é que não tinha corrido bem desta vez" e por ter aceite participar neste projeto com entusiasmo.

À Dra. Maria João Amorim e ao seu grupo no Instituto Gulbenkian de Ciência, por me terem acolhido e ajudado a planear e desenvolver as experiências da infeção.

Ao pessoal do mestrado e a todas as pessoas que conheci em Aveiro, obrigada por terem descoberto esta cidade comigo, pelas horas de maluqueira e desespero. Foram sem dúvida imprescindíveis nessa etapa!

Ao Daniel, pela força, pela companhia e por me dares ânimo para ultrapassar os momentos menos bons. Obrigada por acreditares em mim e nos meus "primers".

À minha família. Aos meus pais, ao meu irmão, aos meus avós, aos meus tios, um obrigado muito especial. Por sempre se mostraram presentes e interessados no meu trabalho, e por terem feito o que podiam para me ajudar a terminar esta etapa com sucesso.

Also, I want to sincerely thank to Daniela and Prof. Dr. Wolfram Brune for giving me the opportunity to spend some time in Hamburg. It was definitely a great experience that allowed me to meet wonderful people that shared with me their experience in the lab and also a lot of curiosities from their different cultures and interests.
Lastly, I want to thank to my roommates and to the people I met there, for making me miss Hamburg the way I do.

palavras-chave

Infeção viral, Vírus da Influenza A, Citomegalovírus, Dinâmica de Organelos, Peroxissomas, Mitocôndrias, Proteostase, Imunidade Inata

resumo

Os vírus são agentes infeciosos oportunistas. Os diferentes passos de um ciclo de vida viral, incluindo a entrada do vírus na célula, a replicação do seu genoma e a formação de novas partículas virais requerem interações com os diferentes componentes celulares do hospedeiro, nomeadamente com organelos. Neste projeto, propomos estudar dois tipos diferentes de vírus que afetam dois mecanismos distintos de sobrevivência celular: a influência do Citomegalovírus de humano (HCMV) na resposta imunitária inata e o efeito do Vírus da Influenza A (IAV) na proteostase.

O HCMV pode estar associado com consequências graves para a saúde da população, uma vez que tem a capacidade para estabelecer uma infeção latente e persistente no hospedeiro. Este vírus codifica para a vMIA, uma proteína anti-apoptótica que se localiza nos peroxissomas e nas mitocôndrias, induzindo a sua fragmentação e inibindo a resposta antiviral celular que é estabelecida em ambos. Com isto, sugerimos mapear os domínios da vMIA responsáveis pelas alterações na morfologia dos organelos e na inibição da resposta imune. Os nossos resultados revelaram que a sequência de aminoácidos 115-130 poderá ser importante para a fragmentação dos organelos. Também descobrimos que a proteína m38.5 do Citomegalovírus de ratinho (MCMV), análoga à vMIA, parece localizar nos peroxissomas, induzir a sua fragmentação e claramente inibir a resposta antiviral dependente deste organelo. Estes resultados sugerem que este vírus poderá ser útil para complementar os nossos resultados com experiências animais ou no contexto de infeção viral.

O IAV é o agente causativo da maioria das epidemias anuais em humanos. Durante a infeção com IAV, ocorre acumulação de proteínas com conformação errada e a formação de locais especializados de replicação viral, resultando na formação de agregados insolúveis ou inclusões. Neste estudo, propusemos determinar se a infeção com IAV conduz à acumulação de proteína com pré-disponibilidade para formar agressomas. Os nossos resultados, embora preliminares, sugerem que existe formação destas estruturas durante a infeção viral, previamente à libertação do genoma viral no citoplasma.

keywords

Viral infection, Influenza A Virus, Cytomegalovirus, Organelle Dynamics, Peroxisomes, Mitochondria, Proteostasis, Innate Immunity

abstract

Viruses are small opportunistic infectious agents. Virus entry, replication and assembly are dynamic and coordinated processes that require precise interactions with host components, often with cellular organelles. Hence, we proposed to study two different viruses affecting two distinct cellular surveillance mechanisms: Human Cytomegalovirus (HCMV) and Influenza A Virus (IAV) influence on the innate immune response and proteostasis, respectively.

HCMV might be associated with additional long-term health consequences in human due to its ability to establish a lifelong persistent latent infection. HCMV encodes vMIA, an anti-apoptotic protein known to co-localize at peroxisomes and mitochondria, induce their fragmentation and inhibit the downstream cellular antiviral response that is established at both organelles. In the present work, we aimed to characterize the role of vMIA in the peroxisomal-MAVS dependent antiviral response. We proposed to map the vMIA domains responsible for the organelles' morphology changes and innate immune response inhibition. Our results revealed that the 115-130 amino acid sequence might be important for the organelles' fragmentation. We also found that m38.5, an analogue of vMIA in murine CMV (MCMV) seems to localize at peroxisomes, induce the organelle's fragmentation and clearly inhibit the peroxisome-dependent antiviral immune response. These results suggest that this virus may be useful to complement our results with experiments performed in animals or in the context of a viral infection.

IAV is the causative agent for most of the annual epidemic in humans. During IAV infection, it occurs the accumulation of unfolded proteins and the formation of specialized sites of viral replication, resulting in the formation of insoluble aggregates or inclusions. In this study, we proposed to determine whether and how IAV infection leads to aggresomal-prone proteins accumulation. Our preliminary results suggest aggresomes formation during viral infection, previous to the vRNP release in to the cytoplasm.

List of abbreviations

ATF4/6	Activating Transcription Factor 4/6
ATF6f	ATF6 fragment
ATP	Adenosine Triphosphate
Bid	BH3 interacting-domain death agonist
BIP	Binding Immunoglobulin Protein
c/EBP	cAMP response Element-Binding Protein
cAMP	cyclic Adenosine Monophosphate
CARD	caspase activation and recruitment domains
CARDIF	CARD adaptor inducing IFN-β
cGAMP	cyclic GMP-AMP synthase
cGAMP	cyclic Guanosine Monophosphate–Adenosine Monophosphate
cGAS	cGAMP Synthase
CHOP	C/EBP Homologous Protein
CLRs	C-type Lectin Receptors
CMV	Cytomegalovirus
cRNA	complementary RNA
DAMPs	Damage-Associated Molecular Patterns
DLP/DRP1	Dynamin-Like Protein/Dynamin-Related-Protein GTPase
DNA	Deoxyribonucleic Acid
dsDNA	double stranded DNA
EGFR	Epidermal Growth Factor Receptor
eIF2α	eukaryotic Translation Initiator Factor 2α
eIF4	eukaryotic Initiation Factor 4
ER	Endoplasmic Reticulum
ERAD	ER-associated degradation
FADD	FAS-associated Death Domain Protein
FasR	FAZ receptor
FDA	Food and Drug Administration
FIS1	Fission Protein 1
gB/gH	glycoprotein B/H
GDAP1	Ganglioside-Induced Differentiation-Associated Protein
GTP	Guanosine-5'-Triphosphate
HA	Hemagglutinin
HCMV	Human Cytomegalovirus
HDAC6	Histone Deacetylase 6
HHV-5	Human Herpesvirus 5
HIV	Human Immunodeficiency Virus
HSF1	Heat Shock Factor 1
HSPs	Heat Shock Proteins
IAV	Influenza A virus
ICTV	International Committee on Taxonomy of Viruses
IFN	type-I Interferons
IPS-1	IFN-β Promoter Stimulator

IRE1	Inositol-Requiring Enzyme 1
IRF	Interferon Regulatory Factor
ISGF	Interferon-Stimulated Gene Factor
ISGs	IFN-Stimulated Genes
JAK-STAT	Janus Kinase-Signal Transducers and Activators of Transcription
JNK	c-Jun N-terminal kinase
kbp	kilo base pairs
kDA	kilo Daltons
LE	Late Endosome
LGP2	Laboratory of Genetics and Physiology
MAMs	Mitochondria-Associated Membranes
MAVS	Mitochondrial Anti-Viral Signalling
MCMV	Murine Cytomegalovirus
MDA5	Melanoma Differentiation-Associated Gene-5
MDVs	Mitochondria-Derived-Vesicles
MFF	Mitochondrial Fission Factor
MOMP	Mitochondrial Outer Membrane Permeabilization
mRNA	messenger RNA
MTOC	Microtubule Organizing Centre
NA	Neuraminidase
NF-κB	Nuclear Factor kappa B
NLR	NOD-Like Receptors
NLS	Nuclear Localization Sequences
NOD	Nucleotide-binding Oligomerization Domain
NP	Nucleoprotein
NPC	Nuclear Pore Complex
NS1A/NS2	Non-Structural Protein
ORF	Open Reading Frame
PA	Polymerase Acidic Protein
PAMPs	Pathogen-Associated Molecular Patterns
PB1/2	Polymerase Basic Protein 1/2
PERK	PKR-like ER kinase
Pex	Peroxin
PKR	Protein Kinase RNA
PMP	Peroxisomal Membrane Protein
PRR	Pattern-Recognition Receptors
RD	Repressor Domain
RdRP	RNA-dependent RNA polymerase
RIDD	Regulated IRE1-dependent mRNA decay
RIG-I	Retinoic Acid-Inducible Gene-I
RIPK1	Receptor Interacting Protein Kinase-1
RLRs	RIG-I-like Receptors
RNA	Ribonucleic Acid
ROS	Reactive Oxygen Species
ssRNA	single strand RNA
STING	Stimulator of Interferon Genes

sXBP1	spliced XBP1
t-Bid	truncated Bid
TLRs	Toll-like Receptors
TNF	Tumor Necrosis Factor
TRADD	TNFR-associated Death Domain Protein
TRAF	TNF Receptor-Associated Factors
TRAIL	TNF-Related Apoptosis-Inducing Ligand
TRAILR	TRAIL Receptor
$tRNA_i^{Met}$	transfer RNA methionine initiator
UPR	Unfolded Protein Response
UPS	Ubiquitin-Proteasome System
vICA	viral Inhibitor of Caspase-8 Activation
VISA	Virus-Induced Signaling Adaptor
vMIA	viral Mitochondria-Localized Inhibitor Of Apoptosis
vRNA	viral RNA
vRNPs	viral Ribonucleoprotein complexes
WHO	World Health Organization
XBP1	X Box-Binding Protein 1

Index

CHAPTER I Human Cytomegalovirus and Innate Immunity **1**
1.1 Human Cytomegalovirus **3**
1.2 Epidemiology **3**
1.3 Genome and morphology **4**
1.4 Life cycle **4**
  Treatment 6
1.5 Antiviral innate immune sensing **6**
  Tool-like receptors 6
  Cyclic GMP-AMP synthase (cGAS) 7
  RIG-I-like receptors (RLRs) 7
1.6 RIG-I-MAVS signaling **8**
1.7 Virus-induced apoptosis **10**
1.8 vMIA’s dependent CMV evasion from antiviral cellular responses **11**
  Organelle’s morphology and RIG-I-MAVS signaling 11
  Apoptosis 13
CHAPTER II Influenza A Virus and Proteostasis **15**
2.1 Influenza A virus **17**
  Epidemiology 17
2.2 Genome and morphology **17**
2.3 Replication cycle **18**
2.4 Treatment **21**
2.5 Proteostasis and Quality Control Machinery **21**
2.6 Protein aggregation and aggresome formation **23**
2.7 Unfolded protein response **25**
  Influenza A virus infection and UPR^{ER} inducing 27
CHAPTER III Aims of the study **29**
  Human Cytomegalovirus and Innate Immunity 31
  Influenza A Virus and Quality Control Machinery 31
CHAPTER IV Materials and Methods **33**
4.1 Materials **35**
  4.1.1 Cell lines 35
  4.1.2 Cell Culture Solutions 35
  4.1.3 Bacterial strains 35
  4.1.4 Bacterial Media 35
  4.1.5 Viruses 36
  4.1.6 Plasmids 36

4.1.7 Vectors 36
4.1.8 Primers and Oligonucleotides 36
4.1.9 Transfection Reagents 37
4.1.10 Markers and Loading Dyes 37
4.1.11 Enzymes 37
4.1.12 Kits 37
4.1.13 Antibodies 38
4.1.14 Solutions and Buffers 38
4.1.15 Databases and Software 39
4.2 Methods 40
4.2.1 Cell Culture 40
4.2.2 Transformation of competent bacteria 40
4.2.3 Transient Mammalian Cell Transfection Methods 42
4.2.4 Immunocytochemistry 42
4.2.5 Reverse transcriptase - quantitative Polymerase Chain Reaction (PCR) 43
4.2.6 Infection 45
4.2.7 Immunobloting 45
4.2.8 Quantification methods 46
4.2.9 Clustered Regularly Interspaced Short Palindromic Repeats/CRISPR associated system 9 (CRISPR/Cas9) for gene knockout 47
4.2.10 Statistical Analysis 48
CHAPTER V Results and Discussion 49
5.1 Human Cytomegalovirus and Innate Immunity 51
Mapping the vMIA domains responsible for organelles' morphology change 51
Mapping the vMIA domains responsible for the inhibition of innate immune response 54
Creation of a PEX19 KO cell line 55
Study of the vMIA analogue in MCMV 56
5.2 Influenza A Virus and Quality Control Machinery 59
CONCLUDING REMARKS 63
Human Cytomegalovirus and Innate Immunity 65
Influenza A Virus and Quality Control Machinery 65
Publications resulting from this work 67
REFERENCES 69

List of figures

Figure 1 Schematic representation of HCMV structure. 4
Figure 2 Schematic representation of HCMV life cycle in a human cell.. 5
Figure 3 Organelle-Specific MAVS Signaling. 9
Figure 4 Representation of vMIA anti-apoptotic domains. 11
Figure 5 Representation of mitochondrial (A) and peroxisomal (B) growth and division in mammalian cells. 12
Figure 6 Inhibition of apoptosis by CMV.. 14

Figure 7 Schematic representation of IAV virion. 18
Figure 8 IAV life cycle 20
Figure 9 A schematic representation of the cellular quality control machinery involved in the maintenance of proteostasis. 22
Figure 10 IAV hijacks aggresome processing machinery during virus entry. 24
Figure 11 Schematic representation of UPR pathway. 26
Figure 12 Reverse transcription PCR cycle of cDNA synthesis. 43
Figure 13 PCR cycle used to amplify GAPDH gene. 44
Figure 14 RT-qPCR cycling protocol. 45
Figure 15 Structural and functional characterization of vMIA and different sequence-deletion vMIA mutants. 52
Figure 16 Peroxisomal morphology and vMIA mutants localization in MAVS PEX cells.. 53
Figure 17 Deletion mutants of vMIA inhibit the peroxisome-dependent innate immunity signaling. 54
Figure 18 Complementary characterization of vMIA and its different mutants.55
Figure 19 Schematic and shorten representation of CRISPR/Cas9 system. 56
Figure 20 CRISPR/Cas9 PEX19 KO cell lines. 56
Figure 21 Peroxisomal morphology and m38.5 localization within transfected MAVS PEX cells.57
Figure 22 m38.5 inhibits MAVS PEX innate immunity signaling. 58
Figure 23 Aggresomal formation in HeLa HSPB1-GFP cells infected with ΔNS1 IAV. 60
Figure 24 Caracterization of insoluble protein fraction upon infection at different time points, normalized to the total fraction. 61
Figure 25 ATF6 is activated upon IAV infection. 62

CHAPTER I

Human Cytomegalovirus and Innate Immunity

Human Cytomegalovirus and Innate Immunity

1.1 Human Cytomegalovirus

According to the International Comittee on Taxanomy of Viruses (ICTV, 2011), cytomegalovirus (CMV) belongs to the subfamily *Betaherpesvirinae*, family *Herpesviridae* and order *Herpesvirales*. It takes part of the Group I of Baltimore's Classification of double stranded desoxyribonucleic acid (dsDNA)[1]. Several species of CMV have been identified and classified for different mammals, being humans and monkeys its natural hosts.

Cytomegaloviruses are widely distributed in nature and are characterized generally by slow growth, restricted species specificity, and by inducing a typical cytopathic effect on infected cells involving specific nuclear and cytoplasmic inclusions as well as cell enlargement. Human herpesvirus 5 (HHV-5), commonly named as Human cytomegalovirus (HCMV), is common in the human population and is becoming increasingly apparent that it might be associated with additional long-term health consequences due to its ability to establish a lifelong persistent latent infection[2]. Murine CMV (MCMV), a natural mouse pathogen, shares a high degree of sequence homology and biology with HCMV, and is a widely used model to study HCMV infection[3].

1.2 Epidemiology

HCMV is a highly widespread pathogen that infects people of all ages, with higher seroprevalence in the elderly, being more common in developing countries and in communities with lower socioeconomic status[4].

Upon primary infection, the virus is intermittently shed in multiple body fluids, hence, transmission can occur via saliva, sexual contact, blood transfusion and solid-organ or hematopoietic stem cell transplantation[5]. Recurrent infection occurs with reactivation of latent virus in response to immunosuppression, or reinfection with a different strain in a seropositive individual for CMV.

Considering an immunocompetent host, primary infection is almost always benign with minimal or no clinical manifestation, yet it can result in horizontal or vertical transmission[6]. Occasionally, healthy individuals develop a self-limited mononucleosis syndrome, sore throat, glandular fever and a mild hepatitis. Howecer, HCMV infection turns into a leading cause of illness and life-threatening in immunocompromised subsets of the population, including patients who are undergoing hemodialysis or receiving immunosuppressive drugs, as well as patients with cancer, HIV-infected, or organ transplant recipients[7,8]. In this setting, CMV serves as a major opportunistic pathogen, being a lifelong burden to immune dysfunction.

Also, HCMV has been described as one of the major causes of congenital disorder, including severe and permanent neurological injury in newborns. Vertical transmission can occur transplacentally, during childbirth, or through breastfeeding[9].

1.3 Genome and morphology

HCMV has a spherical to pleomorphic structure, and is the largest of the eight known human herpesviruses, with 150-200 nm in diameter and a 230 kilo base pairs (kbp) non-segmented genome encoding for over than 200 conventional open reading frames (ORFs).

The HCMV virion (Figure 1) consists of a core containing a long non-segmented linear dsDNA surrounded by a symmetric icosahedral capsid. These components are enclosed into a lipid bilayer envelope derived from the host cell endoplasmic reticulum (ER)-Golgi compartments, that contains at least 20 virus-encoded glycoprotein complexes involved in cell attachment and penetration. Between the envelope and the capsid is an amorphous, proteinaceous asymmetric matrix designated the tegument holding few cellular and viral ribonucleic acid (RNA) and the majority of the virion proteins, which can either have a structural role, a modulatory function of the host cell response to infection or be important for the virion (dis)assembly[10]. In addition to viral DNA, HCMV virions also carry mRNAs into the host cells[11].

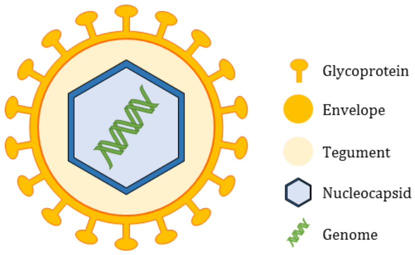

Figure 1 Schematic representation of HCMV structure. The dsDNA genome is surrounded by a symmetric icosahedral capsid and enclosed into a lipid bilayer spiked with at least 20-virus encoded glycoprotein complexes, as gB, gH and gL that mediate virus entry in human cells. In between, there is the tegument, a proteinaceous matrix.

1.4 Life cycle

Virus Entry: Attachment and fusion of infectious particles with the host cell membrane requires interaction of several viral glycoproteins (*e.g.* gB and gH[12]) and cell-surface proteoglycans and receptors (e.g. epidermal growth factor receptor (EGFR) and β1 integrins). HCMV can enter the cells either through endocytosis or direct fusion of the envelope with the cellular membrane (Figure 2, step 1).

After internalization, nucleocapsids, virion mRNA and tegument proteins are released into the cytoplasm (Figure 2, step 2a and 2b), where virion mRNAs are translated. Tegument proteins bound to the capsid are believed to interact with the host microtubule machinery to transport viral capsids to into nucleus, where the genome is released (Figure 2, step 3) and where viral transcription, genome replication and encapsidation occurs[13].

Viral Gene Expression and Replication: HCMV starts to express its genes using the cellular transcriptional machinery. Productive replication leads to the temporal-coordinated synthesis of three classes of proteins, each regulating different aspects of the infectious cycle. Tegument proteins by incoming virions tightly inhibit the initial steps of immune response and initiate the time-dependent cascade of viral genome expression[13].

Immediate early genes (0–4 hours after infection) have been shown to be responsible for the early cytopathic effect, to protect the virus against innate host immunity and be involved in the regulation of transcription. Early viral genes (4–48 hours after infection) are involved in viral DNA replication and further transcriptional regulation. Furthermore, late genes are expressed during the remainder of infection up to viral egress and typically code for structural proteins[14].

When latent, viral genomes take the form of closed circular episome in tandem with the host cell DNA and retain the capacity to replicate using the host cell replication machinery, although being expressed only a small subset of viral genes[15].

Virion assembly and release: Late gene expression drives capsid assembly in nuclear viral factories and nuclear egress to the cytoplasm (Figure 2, step 4). Capsids are then associated with tegument proteins and trafficked to the viral assembly complex, comprised by host's endoplasmic reticulum, Golgi apparatus and endosomal machinery, to acquire a tegument layer and an envelope[13]. Furthermore, cellular and viral RNAs are packaged into virions in proportion to their intracellular concentration[11] (Figure 2, step 5).

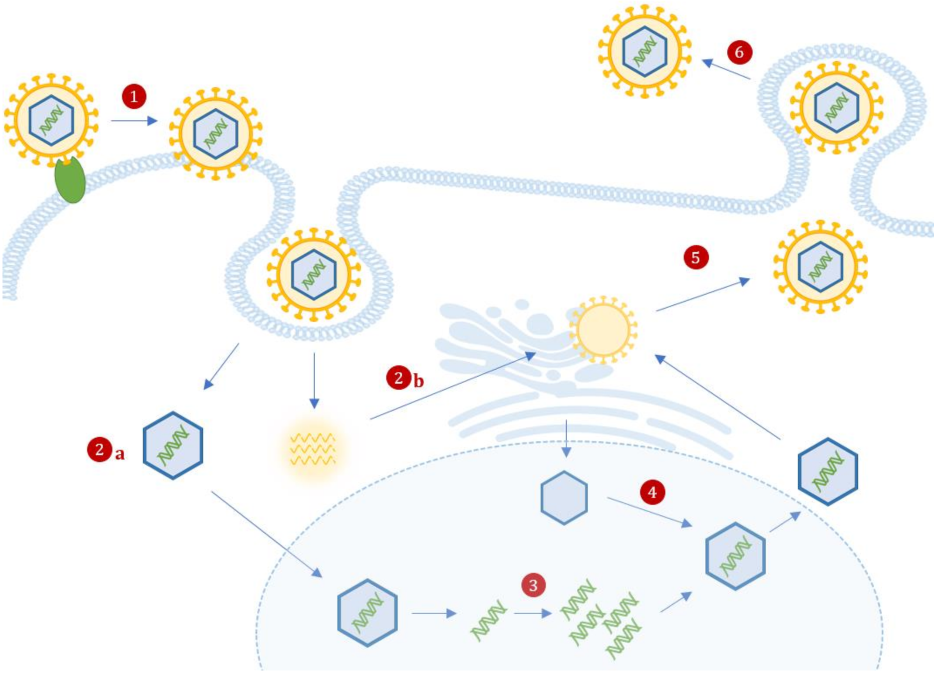

Figure 2 Schematic representation of HCMV life cycle in a human cell. HCMV attaches to the cell via interactions between viral glycoproteins (e.g., gB and gH) and specific surface receptors (e.g. EGFR), and is incorporated either through direct fusion or the endocytic pathway (1), followed by the release of nucleocapsids (2a), viral proteins and viral mRNA (2b) into the cytoplasm. These mRNA are translated and the nucleocapsids are translocated into the nucleus, where viral DNA is released (3), and initiates the expression of IE genes. Viral replication and maturation involves the encapsulation of replicated viral DNA as capsids (4), which are then transported to the cytoplasm. Secondary envelopment occurs in at the ER-Golgi intermediate compartment (5). This is followed by virion release by exocytosis at the plasma membrane (6). Adapted from Crough et al., 2009[16].

Enveloped infectious particles along with non-infectious dense bodies are next released into the extracellular space by exocytosis (Figure 2, step 6). HCMV is a lytically replicating virus, thus after it causes massive cell enlargement, its life cycle culminates with the destruction of the infected cell.

Treatment

The most common treatment for patients with weakened immune system who have HCMV infection symptoms is prophylactic antiviral medication. Currently, all licensed anti-HCMV drugs are nucleoside analogs and all share the same fundamental mechanism of action, namely the inhibition of viral DNA polymerase, and consequently viral replication, being ineffective against a latent virus. In clinical practice, these drugs are frequently used for broader indications related to the treatment and prevention of HCMV infection in immunocompromised hosts[9].

Cytogam®, Cytomegalovirus Immune Globulin Intravenous is an immunoglobulin G containing a consistent number of antibodies to HCMV. Alone or in combination with an antiviral agent, this medication has been approved by Food and Drug Administration (FDA) for the prophylaxis of HCMV disease in high-risk patients having an organ transplant and reduce the risk of HCMV-related diseases and death in some of the highest-risk patients[9,17].

1.5 Antiviral innate immune sensing

The innate immune system on eukaryotic organisms holds very well-defined defense mechanisms against evading pathogens in early phases of infection. The innate antiviral immunity is activated with the detection of evolutionarily conserved structures termed pathogen-associated molecular patterns (PAMPs), by a set of host's germline-encoded pattern-recognition receptors (PRRs). Endogenous products produced during cell damage or tissue destruction upon infection also stimulate PRRs[18,19].

According on their localization, PRRs may be classified into membrane-bound PRRs, that include Toll-like receptors (TLRs) and C-type lectin receptors (CLRs); and cytoplasmic PRRs, including nucleotide-binding oligomerization domain (NOD)-like receptors (NLRs), retinoic acid-inducible gene-I (RIG-I)-like receptors (RLRs), as well as cytosolic viral DNA sensors such as cyclic guanosine monophosphate–adenosine monophosphate (cGAMP) synthase (cGAS)[18]. The recognition of viral PAMPs, that mainly consists of viral nucleic acids, such as 5' triphosphate terminal RNA, is possible due to endosomal TLR, cytosolic DNA sensors and cytosolic RLRs[20].

Tool-like receptors

TLRs are considered the primary sensors of pathogens[19]. TLRs are type I membrane glycoproteins and consist of one extracellular and one cytoplasmic domains, required for PAMP recognition and downstream signaling, respectively. Following TLR activation by PAMPs, a variety of adaptor molecules are activated and induce a signaling cascade that culminates in the activation of transcription factors that will regulate the expression of interferon (IFN), cytokines and chemokines[20].

To date, 10 TLR family members have been identified in humans. TLR1, 2, 4, 5 and 6 are primarily expressed on the cell surface, whether TLR3, 7, 8 and 9 are exclusively expressed within endocytic compartments[20].

HCMV virions were shown to trigger inflammatory cytokine responses via envelope gB and gH recognition by TLR2, in a mechanism dependent of nuclear factor kappa B (NF-κB) activation[21], and were proven to induce TLR4 signaling components and downstream IFN expression[22]. On the other hand, endosomal TLR3 and 9 were demonstrated as essential components in the innate immune defense to MCMV infection[23].

Cyclic GMP-AMP synthase (cGAS)

cGAS is a cytosolic DNA sensor belonging to the nucleotidyltransferase family. Once bound to DNA, cGAS catalyzes cGAMP synthesis, which in turn binds to and activates the ER protein stimulator of interferon genes (STING). This protein is a critical signaling molecule of the innate immune response against DNA viruses, once it further activates the antiviral type I IFN signaling pathway.

It is known that UL122, which encodes the immediate-early 2 86 kilo Dalton (kDa) protein (IE86), strongly abolished cGAMP-mediated type I interferon (IFN) promoter activation, as it facilitates proteasome-dependent degradation of STING[24]. Also, the HCMV tegument protein UL82 was identified as a negative regulator of STING-dependent antiviral responses[25]. Furthermore, STING was described as necessary for the first phase of type I IFN production that limits early CMV replication, proven that the cGAS-STING pathway has a pivotal role in the initial detection of CMV infection[26].

RIG-I-like receptors (RLRs)

RLR family are expressed in most cell and tissue types and consists in three molecules: retinoic acid-inducible gene (RIG-I), melanoma differentiation-associated gene-5 (MDA5) and laboratory of genetics and physiology 2 (LGP2). These sensors recognize the RNA from RNA viruses in the cytoplasm of infected cells and induce inflammatory cytokines and type I interferons.

Structurally, all three members contain an intermediate DExD/H-box RNA helicase domain which is involved in recognition and binding to pathogen nucleotides, as well as adenosine triphosphate (ATP) hydrolysis-involved conformational changes; and a C-terminal repressor domain (RD)[27,28]. RIG-I and MDA5 also contain two N-terminal tandem caspase activation and recruitment domains (CARDs) that are essential for downstream signaling cascade[29,30]. The RD of RIG-I maintains the receptor in a closed, stable and inactive conformation that constrains the activation of the downstream signaling, being necessary its activation via conformational changes to expose its RIG-I CARD to further initiate antiviral signaling. Opposing to RIG-I, MDA5 has the CARD domains permanently exposed[20].

Although RIG-I and MDA-5 have specificities for different ligands, effective sensing of PAMPs rapidly induces host immune responses via the activation of intracellular signaling cascades that ultimately leads to the induction of IFN and IFN-stimulated genes (ISGs), as well as pro-inflammatory cytokines[19,31], which subsequently may function as direct antiviral effectors, preventing viral genome replication, viral particle assembly, or virion release from infected cells, and shape the adaptive immune response[18].

1.6 RIG-I-MAVS signaling

Mitochondrial anti-viral signaling (MAVS), also known as IFN-β promoter stimulator (IPS-1), CARD adaptor inducing IFN-β (CARDIF), and virus-induced signaling adaptor (VISA), is localized in the outer mitochondrial membrane[32], peroxisomes[33] and mitochondria-associated membranes (MAM)[32] . Both peroxisomal and mitochondrial MAVS have specific signaling pathways which result in different but complementing activities[20] and are required for antiviral responses with either temporal or functional differences, which suggest that they may be recruiting distinct subsets of adaptor proteins. The different kinetics of ISG expression induction by peroxisomal and mitochondrial MAVS suggest that more than one mechanism of RLR-induced ISG expression may operate in virus-infected cells[29].

Peroxisomes and mitochondria are ubiquitous organelles present in eukaryotic cells, with remarkably dynamic and high plasticity, capable of moving throughout the cell in a motor protein-dependent manner along cytoskeletal tracks. They continuously adapt their abundance, morphology, distribution, enzyme content and activity, according to the metabolic needs, or physiological changes in their cellular environment upon external stimuli. Peroxisomal and mitochondrial abundance varies according to the cell type and is regulated by organelle formation, half-life, and autophagy-mediated degradation[34,35].

Mitochondria are double membrane-bound organelles containing their own genomes and transcription/translation systems. It can adopt a variety of different shapes that can range from small, spherical compartments of 0.1 to 1μm to elongated tubulo-reticular networks up to 10 μm[34]. Peroxisomes are bordered by a single-membrane that surrounds a granular matrix, are devoid of DNA or protein synthesis machinery and are spread throughout the cytoplasm of most eukaryotic cells[36]. Similarly, its shape and size vary greatly in different tissues, ranging from a spherical to rod-like form and from 0.1 to 0.5 μm in diameter, but they can also appear as elongated tubular organelles and small, tubulo-reticular networks with up to 5 μm, which are frequently associated with lipid droplets[34,37].

Besides cooperating in the establishment of an effective cellular antiviral response, peroxisomes and mitochondria cooperate coordinately in managing diverse metabolic processes in mammals, as maintenance of cellular reactive oxygen species (ROS) homeostasis, fatty acids oxidation, and serve as signaling platforms that modulate diverse physiological and pathological processes including inflammation and cell fate transitions[34].

Fluctuations in organelle abundance can be expected to have significant effects on their functional output, and to adjust organelle quantity in response to changing environmental and developmental stimuli, cells coordinate the formation of new organelles and their subsequent degradation once they are excessive or non-functional.

Upon infection, the recognition and binding of exogenous 5'-ppp panhandle dsRNA structures to RD leads to a conformational switch of RIG-I, which releases the autorepressed CARDs[18] (Figure 3, step 1). Activated RIG-I recruits its downstream adaptor MAVS (Figure 3, step 2). MAVS N-terminal contains a CARD-like domain and a proline-rich region allows MAVS to bind with upstream signaling molecules such as RIG-I and MDA5, through homotypic CARD–CARD-mediated interactions. MAVS activation induces the formation of a detergent-resistant prion fibre-like active aggregates that may involve the CARD domains of several MAVS[38].

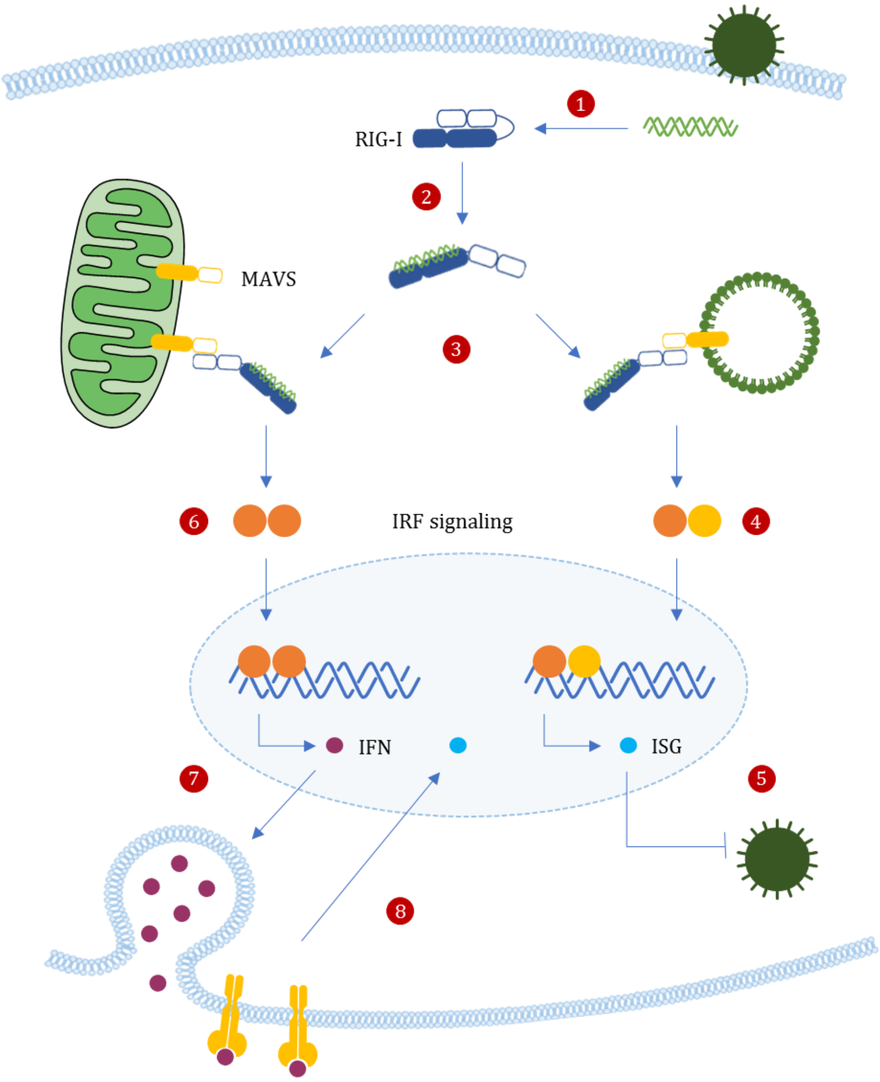

Figure 3 Organelle-Specific MAVS Signaling. Upon infection, detection of exogenous dsRNA structures by RIG-I (1) releases the autorepressed CARDs, leading to its activation (2). Activated RIG-I recruits and bind to mitochondrial and peroxisomal MAVS, through homotypic CARD–CARD-mediated interactions (3). Peroxisomal MAVS was shown is essential for the rapid expression of antiviral genes (ISGs) that will block early antiviral effects, via IRF1 and IRF3 (5). On the other hand, mitochondrial MAVS seems to act with slower kinetics, inducing delayed but sustained responses (6); it promotes type I IFN-dependent ISG expressions, via IRF2, 3 and 6 (7). Once secreted, IFNs bind to specific cell surface type I IFN receptors, leading to the activation of the JAK–STAT pathway, thus generating an amplifying loop leading to RIG-I accumulation during infection and additional ISGs transcription, involved in the generation of the antiviral state (8). Adapted from Sharma et al, 2010[39].

Peroxisomal MAVS was shown to be involved in early rapid, however transient responses, mitochondrial MAVS seems to act with slower kinetics, inducing delayed but long-lasting responses[20,33]. Perhaps the peroxisomal pathway establishes a first outburst of antiviral effector proteins to temporarily block viral replication, while the mitochondrial pathway can induce a stronger and sustained antiviral state although delayed, to clear out the infection[33].

Moreover, peroxisomal MAVS leads to the induction of ISGs via the transcription factors interferon regulatory factor 1 (IRF1) and IRF3, independent of type I IFN production[33], whereas mitochondrial MAVS promote type I IFN-dependent ISG expressions, via IRF2, 3 and 6[20,29](Figure 3). The main advantage of peroxisomal early response is the absence of pro-inflammatory cytokines secretion that would most definitely cause unnecessary cell damage. However, if this fails to control viral infection, the mitochondrial pathway comes into action, stimulating a more powerful and persistent immune response, in an attempt to prevent further viral spread[39].

Once secreted, IFNs bind to specific cell surface type I IFN receptors, leading to the expression of the interferon-stimulated gene factor 3 (ISGF3) through the activation of the Janus kinase-signal transducers and activators of transcritpion (JAK–STAT) pathway. ISGF3 then translocates to the nucleus and coordinates the transcription of hundreds of ISGs including RIG-I, thus generating an amplifying loop leading to RIG-I accumulation during infection and additional ISGs transcription, involved in the generation of the antiviral state[18,29] (Figure 3, step 8).

1.7 Virus-induced apoptosis

Viruses are capable of exploit and reprogram the host metabolism to replicate, what may lead to the host's cell death[20]. Apoptosis, both extrinsic and intrinsic pathways, schematized in Figure 6, can occur in response to cellular stress induced by viral infection[3].

The extrinsic pathway is a major mechanism of host immune clearance of virally infected cells. Death receptors, as tumor necrosis factor (TNF)-related apoptosis-inducing ligand (TRAIL) receptor (TRAILR) and FAS receptor (FasR), can activate initiator caspases, namely caspase-8 and -10, through dimerization mediated by adaptor proteins, such as FAS-associated Death Domain Protein (FADD), TNFR-associated Death Domain Protein (TRADD) and Receptor Interacting Protein Kinase-1 (RIPK1).

The intrinsic pathway of apoptosis requires mitochondrial outer membrane permeabilization (MOMP), with subsequent release of mitochondrial interspaced proteins, as cytochrome c, that promotes the activation of apoptotic caspases. Bcl-2 family proteins function by regulating the integrity of the mitochondrial outer membrane, and comprise three functional subgroups: BH3-only proteins that act as stress sensors and initiate apoptosis; the effector proteins Bax and Bak that mediate MOMP; and pro-survival Bcl-2 proteins that maintain mitochondrial membrane integrity. Bcl-2 proteins have the capacity to bind to Bax and Bak and thus prevent their activation. BH3-only proteins initiate apoptosis by binding to Bcl-2 proteins and thereby releasing Bax and Bak, or by interaction with Bax and Bak and directly catalyze their activation. In healthy cells, Bax and Bak exist as inert monomers, but as apoptosis proceeds the proteins undergo conformational changes resulting in the formation of large homo-oligomers that permeabilize the mitochondrial membrane[3,40].

The extrinsic cell death pathway can intersect with the intrinsic signaling through the caspase-8-mediated cleavage of BH3 interacting-domain death agonist (Bid) to truncated Bid (t-Bid), which translocates to the mitochondria and interacts with Bax and Bak, to induce MOMP.

1.8 vMIA's dependent CMV evasion from antiviral cellular responses

Goldmacher et al[41] demonstrated that CMV infection provides resistance to apoptosis through the viral mitochondria-localized inhibitor of apoptosis (vMIA) protein. This protein is the product of *UL37* exon 1 (pUL37x1) and, besides being an important regulator of viral response to stress[42], it has been additionally shown to induce the release of ER calcium stores[43]. vMIA has two domains that are necessary and sufficient for its anti-apoptotic function (Figure 4) encoded by Tyr5-Leu34 and Asp118 and Arg147 segments[41,44]. Furthermore, the mitochondrial localization signaling is located within the amino acid 2-30 sequence[44,45], and one or several amino acids within the 135-141 segment of vMIA are essential for its interaction with Bax and further apoptosis inhibition[46,47].

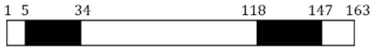

Figure 4 Representation of vMIA anti-apoptotic domains. Adapted from Hayajneh, 2001[44].

Organelle's morphology and RIG-I-MAVS signaling

Upon HCMV infection, vMIA was shown to promote viral replication by efficiently increasing mitochondrial biogenesis in fibroblasts[48]. vMIA is also localized at peroxisomes, interacts with MAVS and specifically diminishes the peroxisomal MAVS-dependent production of ISGs[31].

Mitochondria are continuously remodeled through cycles of fusion and fission[34], whereas peroxisomes have distinct biogenesis pathways. Unlike mitochondria, mature peroxisomes cannot fuse with one another, thus new peroxisomes must arise from division of pre-existing peroxisomes[49] or *de novo* formation[50]. A well-defined sequence of morphological changes, including elongation, constriction, and fission, is most likely the major proliferation process[35].

Both organelles share key components of their fission/division machinery mammals[51], including a dynamin-like protein/dynamin-related-protein GTPase (DLP/DRP1), and its membrane adaptors mitochondrial fission protein 1 (FIS1), mitochondrial fission factor (MFF), and ganglioside-induced differentiation-associated protein (GDAP1). Overexpression or downregulation of their function has been shown to induce its fragmentation or elongation, respectively[35].

DLP/DRP1 is a predominantly cytosolic protein known to function in elongation and fission, not required for organelle constriction. Recruitment of DLP/DRP1 to peroxisomal or mitochondrial division sites depends on FIS1, MFF, and GDAP1 recruitment to organelle membranes. Additionally, peroxisome membrane elongation requires members of the Pex11p family of peroxisomal membrane proteins (PMP) that initiates membrane remodeling and the formation of a tubular membrane extension on one side of the peroxisome[34,52]. This process is schematically represented in Figure 5.

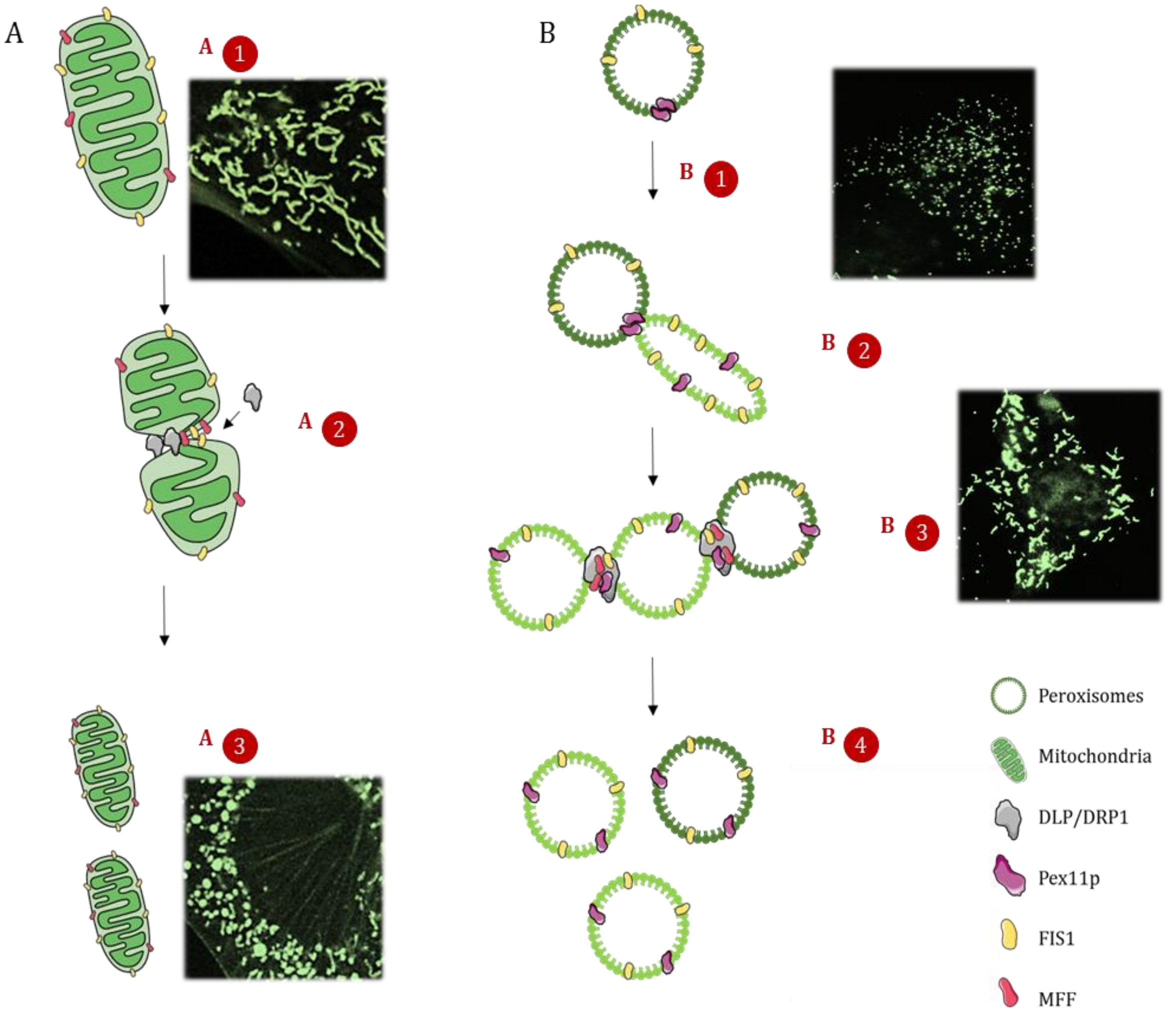

Figure 5 Representation of mitochondrial (A) and peroxisomal (B) growth and division in mammalian cells. A well-defined sequence of morphological changes, including growth/elongation, constriction and fission contributes to organelles proliferation. In Mefs of wild-type cells, mitochondria are characterized by a network of extended tubules (up to 10 µm) distributed roughly throughout the cytoplasm (A1). Replicative mitochondrial fission is initiated by recruitment of cytosolic DLP/DRP1 to the constriction sites, by the adaptor proteins MFF and FIS1, located in the outer mitochondrial membrane (A2). Fragmented mitochondrial appeared mostly as sphere or oval shaped (A3). On the other hand, the activation of Pex11 at pre-existing peroxisomes initiates membrane remodeling and the formation of a tubular membrane extension on one side of the peroxisome (B1). Subsequently, the extension grows and acquires specific set of proteins, as Pex11p and Fis1 (B2). Pex11p and Mff-DLP1 complex concentrate at the sites of constriction (B3). In Mefs, peroxisomes appear as elongated tubular organelles and small tubule-reticular networks (up to 5 µm) and, when fragmented, for instance as a consequence of DLP/DRP1 silencing[31] (B4), they appear significantly smaller and in higher number.

The peroxisomal *de novo* formation might involve the budding and fusion of pre-peroxisomal vesicles derived from the ER or the mitochondrial membrane. It can be explained by a semi-autonomous model of peroxisome formation, whereby the ER and mitochondria supply existing peroxisomes with essential membrane lipids and proteins, including Pex19, Pex3 or Pex16, to allow its growth and division[34,50].

In addition, vMIA had already been shown to induce mitochondrial fragmentation as a necessary step for the inhibition of the mitochondrial-dependent signaling pathway[53,54]. It also induces peroxisomal fragmentation, a mechanism is not essential for vMIA to specifically inhibit signaling downstream the peroxisomal MAVS. Thus, vMIA appears to act at both organelles via distinct mechanisms[31].

Apoptosis

With a slow replication cycle, HCMV depends on the sustained cell viability and, to prevent the premature death of infected cells, the virus is known to block apoptotic signaling pathways and subvert the host antiviral response[31].

Several viral immediate early gene products with antiapoptotic properties have been identified in HCMV, including, UL36, UL37 and UL38, represented in figure 6. The UL36-38 immediate-early locus is highly conserved among HCMV strains and it is required for its replication, once it encodes for proteins that inhibit the ability of an infected cell to activate cell-degrading caspases[44].

The *UL36* gene product is known as vICA (or pUL36), which stands for viral inhibitor of caspase-8 activation. vICA blocks the extrinsic cell death pathway by binding to procaspase-8 and blocking its cleavage and subsequently activation[3].

Furthermore, HCMV deficient for *UL37x1* gene, that encodes for vMIA, has a severe growth defect as a result of strong induction of apoptosis in infected cells[55,56].

vMIA is known to inhibit apoptosis through inactivation of Bax. It binds and sequesters Bax at mitochondria's outer membrane in form of high-molecular weight and inactive oligomers that lacks capacity to induce MOMP[46]. Whether vMIA is capable of inhibiting apoptosis though Bak is still controversial[46,57,58].

Overall, vMIA prevents the formation of the mitochondrial permeability transition pore and inhibit the release of cytochrome c and pro-apoptotic factors into the cytoplasm, thereby preventing the activation of downstream executioner caspases[31]. The functional properties of vMIA's localization resemble those of Bcl-2 family anti-apoptotic proteins. However, vMIA does not possess homology to any BH domains and its function is independent of t-BID low concentrations[55].

Lastly, *UL38* has recently been shown to encode a cytosolic protein pUL38 that suppresses the ER-stress response, by inducing the expression of chaperones through activating transcription factor 4 (ATF4) and suppression of pro-apoptotic c-Jun N-terminal kinase (JNK) activity[3].

MCMV encodes distinct inhibitors of Bax and Bak, m38.5 and m41.1, respectively. m38.5 protein is encoded at analogous position as HCMV vMIA within the respective viral genomes. Although they share little sequence homology, both seem to localize to mitochondria and inhibit Bax in an analogous manner, therefore preventing apoptosis. m38.5 was proposed to be a functional ortholog of vMIA in MCMV[59,60]. A second MCMV-derived inhibitor, m41.1, associates with Bak at the mitochondrial membrane and acts as a viral inhibitor of Bak oligomerization (vIBO) from HCMV. Optimal replication of MCMV depends upon m38.5 and m41.1, whose combined activities maintain mitochondrial integrity[88].

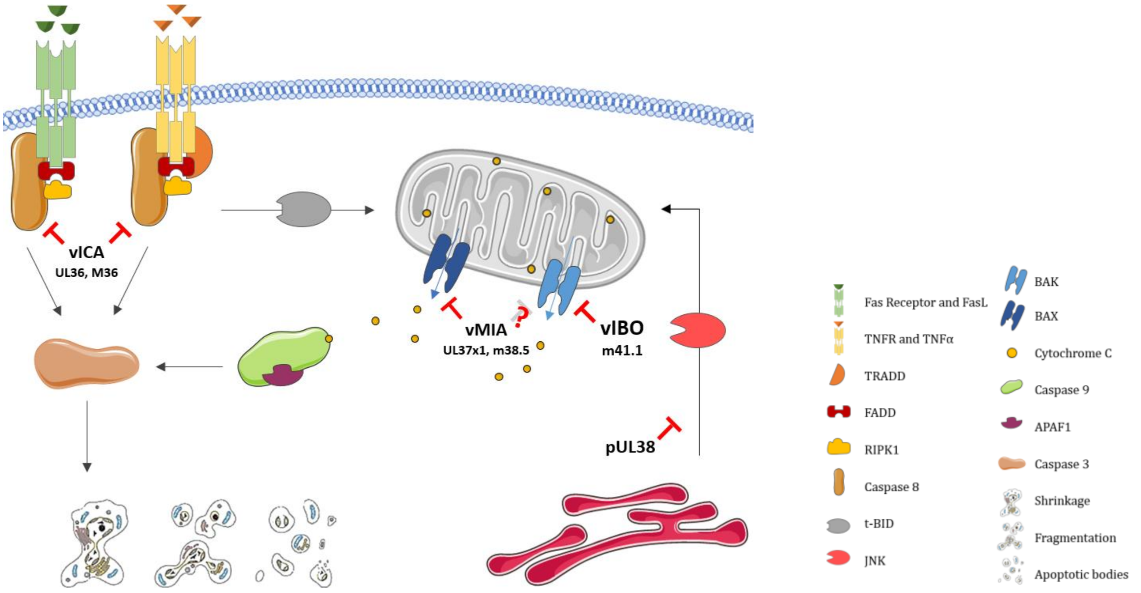
vICA
UL36, M36
vMIA
UL37x1, m38.5
?
vIBO
m41.1
pUL38
Fas Receptor and FasL
TNFR and TNFα
TRADD
FADD
RIPK1
Caspase 8
t-BID
JNK
BAK
BAX
Cytochrome C
Caspase 9
APAF1
Caspase 3
Shrinkage
Fragmentation
Apoptotic bodies

Figure 6 Inhibition of apoptosis by CMV. vMIA and vIBO inhibit MOMP and release of pro-apoptotic factors, as cytochrome c by interacting with BAX and BAK, respectively. MCMV encodes two specific inhibitors, m38.5 and m41.1, HCMV has only pUL37x1, whether the pUL37x1 protein is BAX-specific or inhibits both BAK and BAX is still controversial. The extrinsic apoptosis pathway initiated by death receptors is blocked by vICA, which is encoded by HCMV UL36 and MCMV M36 gene, respectively. APAF1: apoptotic protease activating factor 1; FasL: Fas ligand; FADD: Fas-associated death domain protein; RIPK1: receptor interacting protein kinase-1; TNFα: tumor necrosis factor α; TNFR: TNF receptor; TRADD: TNFR-associated death domain protein; t-BID: truncated BH3-interacting domain death agonist. Adapted from Brune et al., 2017[3].

CHAPTER II

Influenza A Virus and Proteostasis

Influenza A Virus and Proteostasis

2.1 Influenza A virus

Influenza viruses are among the most common viruses causing high morbidity and mortality. Influenza A virus (IAV) has been the causative agent for most of the annual epidemic in humans and the major pandemics of influenza in the last century[61,62].

According to ICTV (2011), IAV belongs to the *Influenzavirus A* genus of the Orthomyxoviridae family that comprises enveloped viruses with segmented, negative-sense single-stranded RNA (ssRNA) genome[62], capable of bind sialic acid in mucoproteins. IAV is designed as a type V virus concerning the Baltimore's classification system[1]. Up to this date, 16 different HA (H1 to H16) and 9 NA (N1 to N9) subtypes have been identified[62], being H1, H2 and H3 the virus subtypes identified in humans.

Epidemiology

Influenza viruses continuously undergo antigenic evolution, either by antigenic drift or antigenic shift. Antigenic drift involves the accumulation of point mutations within the viral RNA genome, particularly in genes that code for antigenic sites. These mutations and the emerging virus strain variants gain selective advantages and evade preexisting immunity, being generally responsible for winter epidemic outbreaks. On the other hand, antigenic shift implies genetic re assortment of RNA segments from different virus strain or different viruses. The new virus subtype arises presenting a novel phenotype with pandemic potential, since there is no immunity to the new virus subtype in the population, allowing the virus to spread rapidly and cause high morbidity and mortality[61].

Both seasonal and pandemic influenza can afflict people of all ages, and most cases will result in self-limited illness in which the person recovers fully without treatment. Seasonal influenza is an acute respiratory disease that is characterized by the sudden onset of high fever, cough, headache and inflammation of the upper respiratory tree and trachea. In the elderly, in infants, and in people with chronic diseases, typical seasonal influenza is associated with especially high risk of developing severe complications within hours, as hemorrhagic bronchitis, pneumonia, and ultimately death in as little as 48 hours after the onset of symptoms[61]. Pandemic outbreaks cause most of its severe or fatal disease in younger people, either in chronic patients and healthy individuals, and caused many more cases of viral pneumonia than is normally seen with seasonal influenza.

2.2 Genome and morphology

The genome of IAV consists of eight single-stranded, negative-sense linear RNA segments (-) ssRNA, encoding for 12 to 14 proteins depending on the strain most of which are necessary for efficient virus replication in host cells and for virion formation. Genome total size is about 3,5kb and the segments size range from 890 to 2341 nucleotides.

The three largest RNA segments encode the three viral RNA-dependent RNA polymerase (RdRP) proteins: polymerase acidic protein (PA), polymerase basic protein 1 (PB1) and PB2. The three intermediate-size RNA segments encode HA, NA and nucleoprotein (NP). The larger of the remaining two segments encodes M1 and M2 matrix proteins, and the smaller one encodes two nonstructural proteins, NS1A and NS2[61,63]. To express spliced forms of viral proteins, as M2 and NS2, the virus uses the host cell's splicing machinery, while prevents the host cell from using it to process host cell messenger RNA (mRNAs), through NS1 interaction with small nuclear RNAs[64].

Each of the eight RNA segments is separately enclosed in the virion in the form of ribonucleoprotein complexes (vRNPs), wrapped in a helical conformation with NP (one subunit binds ~20 nucleotides of vRNA and the vRdRp in both 3' and 5' ends[62].

The influenza virions are known to display many forms, sometimes taking an irregular shape. They are generally spherical or elliptical in shape, ranging from approximately 80 to 120 nm in diameter, and occasional elongated or filamentous, reaching more than 20 µm in length. Regardless of their shape, all virions incorporate an organized set of eight RNPs[62] (Figure 7).

The IAV genome is covered by an envelope coat made up of a lipid bilayer, derived from the host cellular membrane acquired during the budding, that is known to contain both cholesterol-enriched lipid rafts and non-raft lipids. The outer layer of the lipid envelope is spiked with numerous membrane-spanning viral glycoproteins, HA, NA and M2. The type I transmembrane HA is the most abundant envelope protein (~80%), followed by NA (~17%). M2, a highly selective type III transmembrane ion channel, is a very minor component, with only 16 to 20 molecules per virion[64]. The peripheral membrane protein, M1, which is one of the most abundant viral proteins in the virion, binds to the lipid envelope to maintain virion morphology[62].

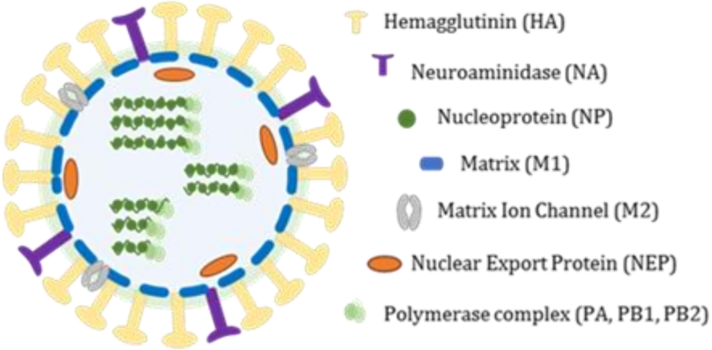

Figure 7 Schematic representation of IAV virion. Eigh (-) ssRNA segments are inclosed into an lipid bilayer envelope spicked with viral glycoproteins.

2.3 Replication cycle

Attachment: The replication cycle begins when the viral surface HA binds to the sialic acid residues from glycoproteins or glycolipids on the host cells membrane[64,65] (Figure 8, step 1). The specificity of HA binding between species depends on the nature of the glycosidic linkage between the terminal sialic acid and the penultimate galactose residue on the receptor. Human influenza viruses preferentially bind to sialic acids attached to galactose in an α (2,6) configuration[64].

Entry into host cell: After successful binding, virion internalization occurs essentially by receptor-mediated endocytosis and the virus is transported into the cell in an endocytic vesicle (Figure 8, step 2). The low pH in the endosome triggers conformational changes in the HA protein, which leads the fusion between the viral envelope and the endosomal membrane[63,64], with the formation of a fusion pore through which the viral genetic material is released. It also stimulates the proton flow into the virus via M2, which then weakens the interaction between the M1 and the vRNPs, promoting their dissociation.

Nuclear transport: After being released into the cytoplasm, the vRNP are transported to the nucleus (Figure 8, step 3) by cellular nuclear import machinery recognition of the nuclear localization sequences (NLS) present in ribonucleoproteins[63], where it undergoes transcription and replication processes.

Transcription and Replication: The (-) vRNA strand is used for the synthesis of capped, polyadenylated mRNAs, a readable form that it is further converted into proteins through process termed *cap-snatching*; and full-length positive sense (+) complementary RNA (cRNA), that will serve as template to produce more (-) vRNA strands to be then packed into the new virions. Both processes are carried out by the viral RdRp enzyme and, due to its short proteasome, the virus hijacks the host transcription machinery for its own purposes.

During the *cap-snatching* process, short oligomers from host pre-mRNA are recognized and bound by the viral PB2 subunit[66], cleaved at the 5' end by the PA endonuclease domain[67] and then used to prime mRNA synthesis via PB1 subunit[68,69]. The viral genome is thereby transcribed using host capped mRNA segments as primers for initiation of viral mRNA synthesis, which ultimately leads to the synthesis of capped translatable viral mRNAs[63]. On the other hand, viral genome replication involves unprimed synthesis of an exact full-length copy of the (-) vRNA into (+) cRNA, which lacks both the 5' capped primer and 3' polyadenylation tail and can be used as templates for further (-) vRNA synthesis further used in the assembly of vRNA complexes[69,70].

NP molecules are required for both steps of replication and are deposited on the cRNA and vRNA during RNA synthesis. Both NP and the RNA polymerase components are complexed with newly synthesized vRNA to form vRNPs[69].

Nucleus export of vRNPs and Translation: vRNPs are exported to the cytoplasm, either for translation into viral proteins and further assembly of new virus particles.

Synthesis and folding of viral core proteins occur entirely in the cytosol, taking advantage of host cell factors to perform viral mRNA translation[70]. The synthesis of viral envelope proteins HA, M2 and NA also starts in the cytosol but are further folded and processed in the host ER and the Golgi apparatus where they undergo post-translational modifications, as glycosylation[63]. Subsequently, the proteins are additionally modified and transported through the trans-Golgi network to the plasma membrane of the cell (Figure 8, step 4).

M1 interact with HA and NA, forming patches with a high density of HA and NA. Subsequently, newly formed RNPs interact actively with the M1 lining at these patches, which prevents re-entry of RNPs into the nucleus and direct them towards the assembly site on the apical membrane of polarized epithelial cells. This ensures that progeny viruses are releases back to the airways. The viral proteins accumulate in the cholesterol rich membrane region named lipid rafts, believed to be the site of virion formation.

Virion assembly: The packaging of vRNPs favors the formation of infectious virus particles with all eight RNA segments required for efficient infection[70] (Figure 8, step 5). After the budding of all viral proteins and vRNP complexes, viral NA cleaves the sialic acid residues on cellular surface glycoproteins or glycolipids, which is bind to HA during the process. Doing that, recently formed virions are released from the host cell's surface (Figure 8, step 6) and start to spread and infection further cells throughout the respiratory tract[64].

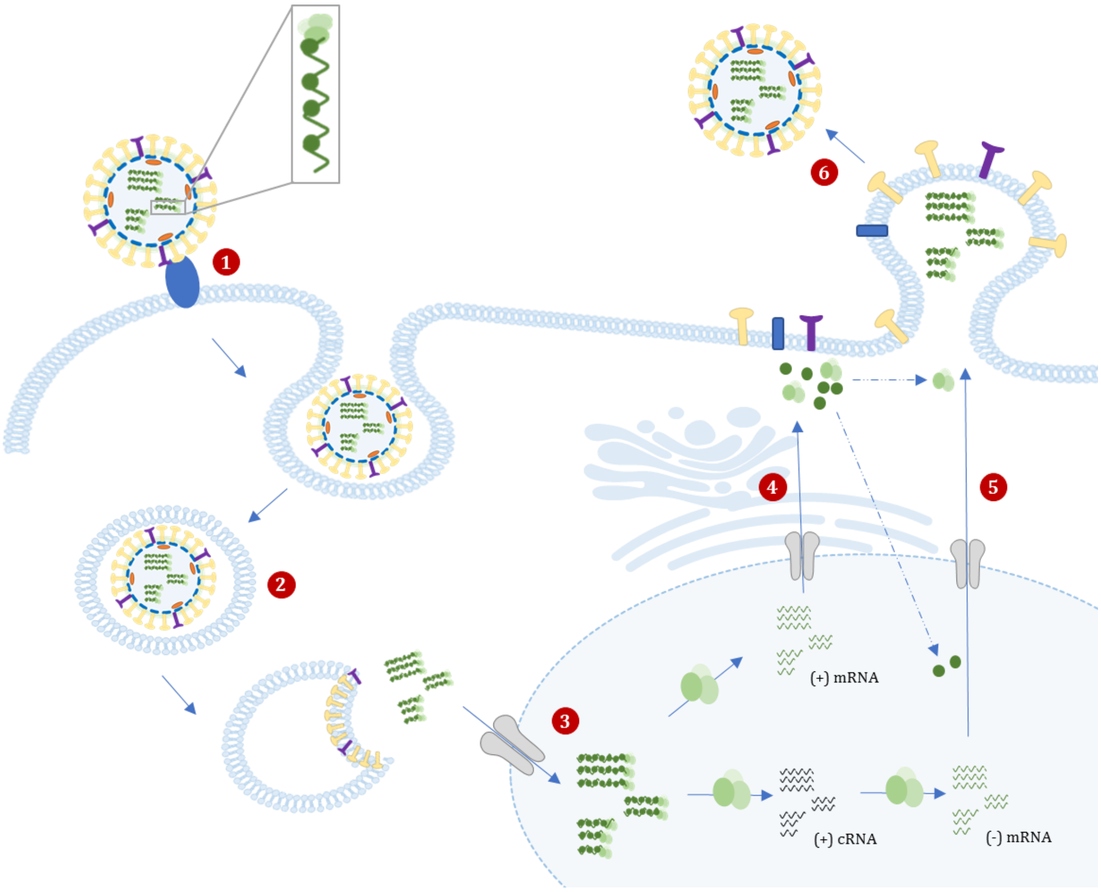

Figure 8 IAV life cycle. The cycle begins when the viral surface HA binds to the sialic acid residues on host cells membrane (1). IAVs is predominantly internalized by endocytosis and the virus is transported into the cell in an endosome (2). The low pH inside the endosome induces the formation of a fusion pore through which the viral genetic material is released and imported to the nucleus (3), where it undergoes transcription and replication processes. Viral core proteins synthesis occurs entirely in the cytosol, whether viral envelope proteins synthesis suffer further processing in the ER and Golgi apparatus (4), and both accumulate at the host membrane. After the budding of all viral proteins and vRNP complexes (5), recently formed virions are released from the host cell's surface and start to spread and infection further cells (6). Adapted from Das et al., 2010[63].

As an acute lytic viral infection, the entire process seriously disrupts the normal physiology of the infected cell and causes the destruction of its membrane, and consequently cell death and desquamation of the respiratory epithelium. However, cell lysis does not occur until the cell has produced many thousands of new virus particles during the latent phase of infection.

2.4 Treatment

Effective measures against influenza A diseases include prevention of infection by either administration of antiviral drugs or vaccination. Antiviral drugs can have both therapeutic and prophylactic effects, but to prevent disease they must be administered continuously at times of high influenza activity[61]. Oseltamivir (Tamiflu®) is a selective NA inhibitor that induces the aggregation of viral particles on the host cell surface, preventing the release and spreading of the new progeny viruses[71]. Amantadine, a M2 ion channel blocker, slows the dissociation of M1 from the RNPs and the viral membrane, inhibiting subsequent steps in the viral life cycle[72].

Nevertheless, vaccination is still the primary strategy for prevention and control of influenza virus, and both inactivated and attenuated vaccines are effective. Once virus subtypes are distinguishable serologically, and the continuous viral antigenic drift of IAV makes once effective vaccines ineffective after a few years' time, having the requirement for regular updates of the composition of the influenza vaccine and annual revaccination is thus recommended for those at high risk[61].

2.5 Proteostasis and Quality Control Machinery

To be functional, most proteins go through a succession of folding intermediate states and adopt a defined three-dimensional native structure. A protein is correctly folded if it has attained its native conformation after required co- or post-translational modifications.

During the folding process, partially folded proteins, as folding intermediates and misfolded conformers, expose some hydrophobic domains that are typically hidden in the native structure, which can lead to nonproductive associations and are prone to trigger protein aggregation[73]. Besides, the proteins in the native configuration can undergo unfolding, specially under stress conditions[74].

Misfolded proteins can interfere with normal cellular functions and be potentially toxic. Thus, cellular proteostasis maintenance is imperative to ensure successful development, healthy aging, resistance to environmental stresses and to minimize homeostasis perturbation by pathogens such as viruses. To suppress the formation of protein aggregates, cells have evolved an elaborated quality-control machinery (Figure 9) that can adapt to the severity of protein damage and acts through ensuring the fidelity of transcription and translation, and induction of stress responses[75–78].

Distinct surveillance mechanisms that respond to misfolded and unfolded proteins have been characterized in the cytoplasm, in the ER and in the mitochondria. For instance, various molecular chaperones and/or chaperonins have evolved to assist post-translationally folding of newly synthesized proteins and refolding of proteins damaged by stress and cellular injuries. For what is known, they occur ubiquitously in all cellular compartments that sustain protein synthesis and folding reactions. Also, while small monomeric proteins can fold in their absence *in vivo*, medium- to large-sized multidomain proteins critically require chaperones to undergo a correct fold[79].

Most cellular proteins are folded directly after translation in the cytosol with the assistance of chaperones, foldases and lectines[80] These molecules, mainly the heat shock proteins (HSPs) HSP60 and HSP70[78], bind to and stabilize exposed hydrophobic residues, prevent incorrect intra– and intermolecular interactions between partially folded or unfolded polypeptides, prevent aggregation and promote the refolding of denatured model substrates and the proper formation of noncovalent interactions that lead to the desired folded state[81].

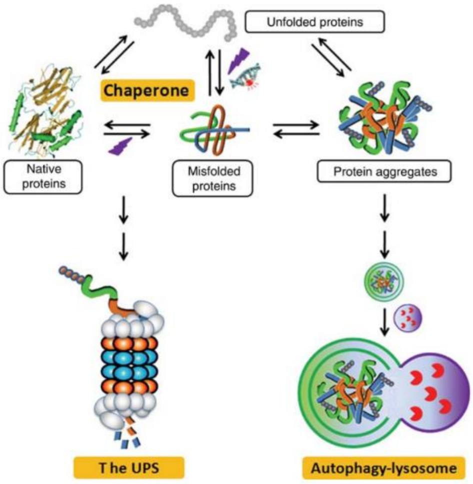

Figure 9 A schematic representation of the cellular quality control machinery involved in the maintenance of proteostasis. Molecular chaperones support the folding of nascent polypeptides and refolding of proteins damaged by stress and cellular injuries. Additionally, they prevent misfolded or unfolded protein from aggregating and escort terminally misfolded protein for UPS degradation. The autophagy-lysosomal pathway aids to remove protein aggregates formed by the misfolded proteins that have escaped from the surveillance of chaperones and the UPS. Adapted from Huabo et al, 2009[82].

Cellular proteins that are unable to fold properly, among non-functional protein fragments and no longer useful proteins, are targeted for degradation by a proteolytic mechanism, termed the ubiquitin–proteasome system (UPS). This system is found in cytosol and nucleus, and mediates degradation of cytosolic, nuclear, secretory and transmembrane proteins. Misfolded secretory and transmembrane proteins are first retained in the lumen or the membrane of the ER, retro translocated back to the cytosol and delivered to the proteasome[83,84]. The UPS involves at first the tagging of misfolded proteins with a polyubiquitin chain, follow by recognition of the polyubiquitylated tag and degradation by the proteasome.

Furthermore, the autophagy-lysosomal pathway helps to remove protein aggregates formed by the aggregation-prone proteins that have escaped from the surveillance of chaperones and the UPS, and defective organelles. First, they are sequestered within an isolated double membrane vesicle, named phagophore, to form autophagosomes, which later fuse with lysosomes to form autophagolysosomes, where the segregated content is degraded by lysosomal hydrolases[85].

2.6 Protein aggregation and aggresome formation

When the amount of misfolded proteins in a cell is so high that exceeds the refolding or degradative capacity of the quality-control machinery, or when the components of the protein homeostasis machinery are disrupted, it leads to the formation and accumulation of insoluble protein aggregates, as a consequence of interaction between aggregation-prone conformers[78,86].

In cells, protein misfolding can be promoted due to specific mutations, RNA modification, translational errors leading to the misincorporation of amino acids, assembly defects of protein complexes or errors during protein folding. Protein aggregates can be either structured, as amyloid, or amorphous. In either case, they tend to be insoluble in aqueous or detergent solvents and metabolically stable under physiological conditions[87].

In a remarkable variety of degenerative diseases, specific proteins have been found to misfold, aggregate and form pathogenic assemblies, ranging from small oligomers to large masses of amyloid. The outcome in all cases is the functional compromise of the nervous system, once the aggregated proteins gain a toxic function and/or lose their normal function[88]. However, progressive formation of protein aggregates is not necessarily pathogenic, as proved by G. Diane Shelton[89], whose results suggested that, although increasing in size with age, aggregates formation was not related with other pathological changes nor functional deficits.

During infection, the formation of specialized sites of viral replication can involve extensive rearrangement of cellular cytoskeleton and membrane compartments, resulting in the formation of insoluble aggregates or inclusions. These aggregates may be part of the innate cellular response that recognizes and sequesters viral components[90], or possibly will be used by viruses as scaffolds for anchoring either viral and host proteins required for replication and assembly, and as a protection from host defense[91].

It is conjectured that upon infection, early-induced aggregates, commonly designated as virus factories, viroplasm or viral inclusions, indicate sites within perinuclear areas that comprises viral genome and proteins involved in virus replication and assembly; and later during infection, these inclusion bodies are thought to either form virus factories and/or arise from the accumulation of viral proteins that do not become incorporated in the virus at other sites in the cell[91].

The term ‘inclusion bodies’ has been applied to refer to the intracellular foci into which aggregated proteins are sequestered. The formation of cytoplasmic inclusion bodies in mammalian cells requires active, dynein-based retrograde transport of misfolded protein on microtubules[92]. Microtubule-dependent cytoplasmic inclusion bodies are generally termed aggresomes.

Aggresomes are not permanently present in the cell. The initial aggregation process is likely to occur co-translationally. If nascent peptides cannot fold correctly, they will co-aggregate to form a single aggresomal particle throughout the cytoplasm. Very quickly after their formation, aggresomal particles are transported towards the microtubule organizing center (MTOC), where they are sequestered into the aggresome[92].

Aggresome formation is initiated by the formation of smaller aggregates in the periphery, which then move in a dynein-based manner along the microtubule cytoskeleton to the final perinuclear site at the MTOC, implying that it is an aggregate of aggregates[86]. Their overall structure and size depends both on the aggregating substrate and the host cell. However, most aggresomes appear as a single sphere of 1-3µm diameter or as an extended ribbon, enriched in components of molecular chaperones and proteasome components[86], and are surrounded by a cage-like vimentin structure contribute to their stability[92].

Transportation machinery involves a microtubule-associated deacetylase, histone deacetylase 6 (HDAC6), a cytoplasmic enzyme that promotes autophagic clearance of protein aggregates and protect cells from cytotoxic accumulation of misfolded proteins (Figure 10). It functions as an adaptor that binds polyubiquitin chains of substrates and the microtubule motor protein dynein, thereby mediating the transport of polyubiquitylated cargo along microtubules towards the MTOC during aggresome formation[93].

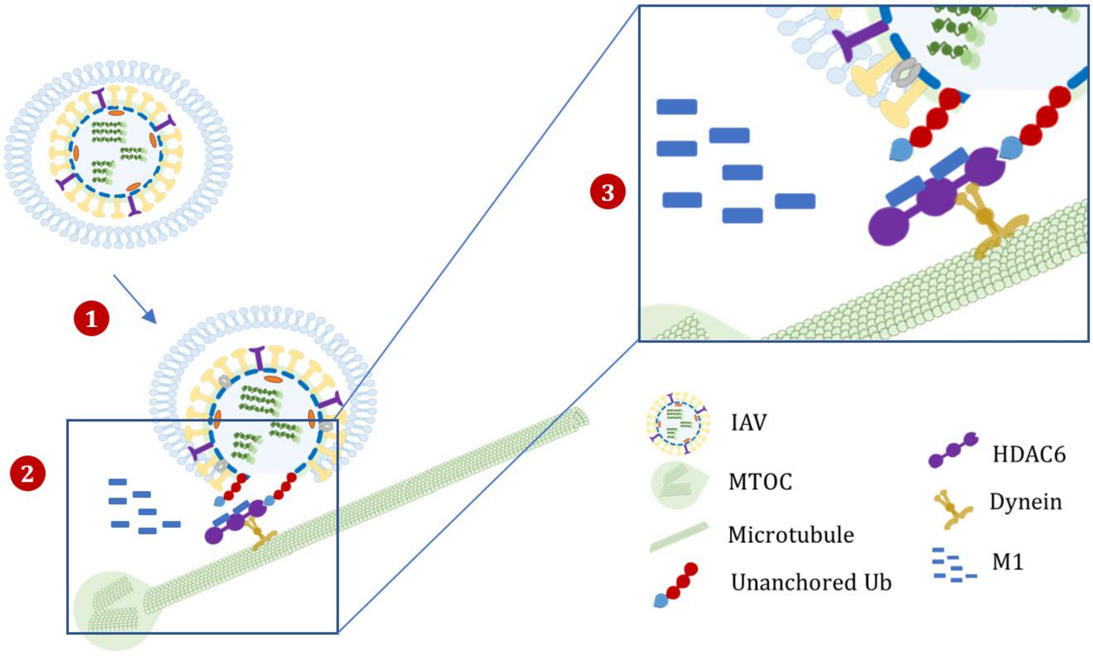

Figure 10 IAV hijacks aggresome processing machinery during virus entry. IAV hijacks endocytosis, travels to late endosomes in the vicinity of the MTOC (1). In LEs the low pH (5.5–5.0) triggers HA acidification and fusion of the viral envelope with endosomal membrane (2). The fusion pore exposes the viral core containing unanchored ubiquitin (Ub) chains to the cytosol (3), inducing a mechanism similar to aggresome processing. Adapted from Rudnicka et al., 2016[94].

IAV requires HDAC6 ubiquitin-binding function, taking advantage of the aggresome processing machinery for host cell entry and especially for capsid uncoating[94,95]. The fusion pore formed between the viral envelope and the endosomal membrane during the IAV life cycle exposes the viral core that contains unanchored ubiquitin chains to the cytosol, which recruit HDAC6 and activate the aggresome processing machinery. HDAC6 binds to matrix protein M1, dynein, and myosin, and promotes capsid disassembly and uncoating: M1 becomes dispersed in the cytosol and the vRNPs are released and further imported to the nucleus[94]. Therefore, unanchored ubiquitin carried by IAV might activate HDAC6 similar to aggresome processing. This mechanism is briefly represented in Figure 10.

2.7 Unfolded protein response

The unfolded protein response (UPR) is a wide range of integrated signaling pathways that act as a stress response mechanisms to cope with conditions of stress at the cellular or organelle-specific level[80,96].

The UPR in the ER (Figure 11) is induced when homeostasis is disrupted by imbalances of protein folding demand and ER-dependent folding capacity[97]. ER proteostasis perturbations, as a consequence of protein overexpression, viral infections, glucose starvation, disturbance of intracellular calcium, oxygen deprivation, toxic exposure and changes in redox state[98–101], may lead to accumulation of unfolded proteins and its aggregation within the ER, which induces ER stress.

In eukaryotic cells, the ER is a dynamic tubular network involved in protein homeostasis, metabolic ATP-demanding processes, such as gluconeogenesis and biosynthesis of phospholipids, and calcium buffering[102,103]. In the ER lumen, proteins are processed and modified into their native conformation, in order to be directed and delivered to their proper target sites within the secretory pathway, displayed on the cell surface or released extracellularly[96,104]. As an organelle for folding and modifications of proteins, the ER is loaded with extremely high concentration of proteins (>100 mg/ml), at which co-aggregation between proteins and/or polypeptides is clearly promoted. Therefore, the lumen of the ER needs a unique cellular environment that promotes processing and prevents aggregation[105].

In the ER, UPR is mediated by three main sensors that reside in the ER membrane: inositol-requiring enzyme 1 (IRE1), double-strand RNA-activated protein kinase RNA (PKR)-like ER kinase (PERK) and activating transcription factor 6 (ATF6), each of which have luminal domains that detect misfolded proteins in the ER and cytoplasmic effector domains that transduce signaling to the transcriptional or transductional apparatus[100].

UPR induces temporally coordinated mechanisms, allied to the expansion of the ER membrane network and simultaneous induction of the expanded organelle space filling with newly synthesized protein-folding and quality control complexes[103,104]. In resting cells, these three sensors are maintained in inactive states through interaction with the binding immunoglobulin protein (BiP) via their luminal domain[102]. During stress, BiP dissociates from these sensors as it is recruited by unfolded proteins to assist their folding. The cytosolic sides from the sensors are auto-activated by trans-phosphorylation[102].

IRE1 is a multi-domain type I transmembrane glycoprotein that has both kinase and RNase activities[99,100]. solely activated by ER stress[105]. When the cytosolic RNase domain is triggered, it can produce either adaptive or death signals[103], via regulated IRE1-dependent mRNA decay (RIDD) and unconventional splicing of the transcription factor X box-binding protein 1 (XBP1) mRNA[99].

RIDD is constitutionally active once it is necessary for ER homeostasis maintenance, and upon stress rises proportionally with its intensity and duration. On the other hand, XBP1 mRNA splicing is activated transiently upon ER stress during the adaptive/pro-survival phase, if RIDD is insufficient to maintain ER homeostasis. The active spliced XBP1 (sXBP1) mRNA controls the expression of genes related to UPR, as chaperones and ER quality control machinery, and modulates phospholipid synthesis, which is required for ER membrane expansion during ER stress[100,103].

If these measures succeed, ER homeostasis is restored and IRE1 oligomers disassemble concomitantly with IRE1 dephosphorylation. Yet, after prolonged and unmitigated exposure to stress, XBP1 mRNA splicing decreases whereas RIDD continues to increase and ultimately induces apoptosis[99]. Overall, in mammals, XBP1 splicing is overactive in cancer with a pro survival output, while RIDD is associated with a pro-apoptotic output in diabetes[99].

PERK is a type I transmembrane membrane which the main function is to modulate translation[106], trough eukaryotic translation initiator factor 2α (eIF2α) phosphorylation.

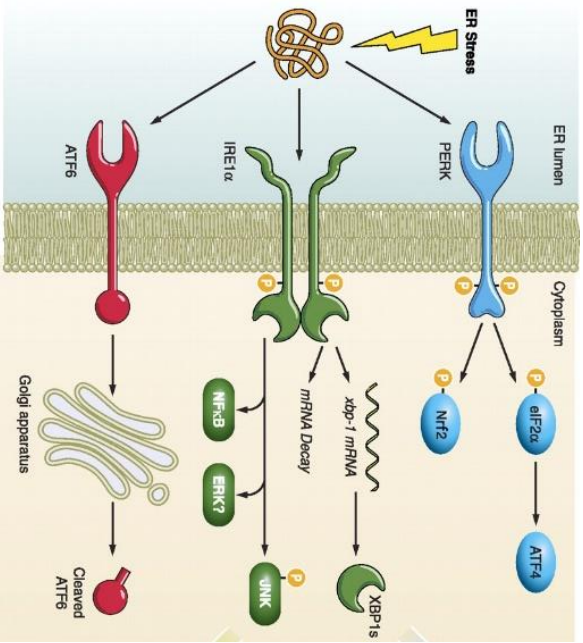

Figure 11 Schematic representation of UPR pathway. ER stress/induced protein imbalance activates the three UPR sensors that culminate into translation attenuation, chaperone induction and aggregation-prone proteins degradation.

eIF2α is the regulatory subunit of eIF2 that under normal conditions is required in the initiation of mRNA translation[102]. Upon phosphorylation, eIF2α subunit indirectly inhibits the guanine nucleotide exchange factor, which normally is necessary to form the tertiary complex with guanosine-5'-triphosphate (GTP) and transfer RNA methionine initiator (tRNA$_i^{Met}$) that initiates translation[98]. That way, it reduces the formation of translation initiation complexes, mRNA translation is inhibited and protein synthesis is attenuated, reducing the flux of protein into the ER[104,106].

However, there are some mRNAs capable of avoiding the eIF2α translational blockage[102,103]. One of these encodes the activating transcription factor (ATF4) that drives the expression of both cyclic adenosine monophosphate (cAMP) response element-binding transcription factor (C/EBP) with pro-survival functions and C/EBP homologous protein (CHOP), a pro-apoptotic factor[104].

Lastly, ATF6 is an activating transcription factor synthetized as an ER-resident type II transmembrane protein with an ER stress-sensing luminal domain and a cytosolic N-terminal DNA binding domain[102]. In cells undergoing ER stress, ATF6 is packaged into ER transport vesicles and delivered into Golgi apparatus[104], where it is sequentially cleaved into an active cytosolic fragment (ATF6f) that corresponds to its DNA binding domain[98,103]. ATF6f is then translocated to the nucleus to activate the transcription of UPR genes, namely chaperones, being the main outcome is the improvement of the ER folding capacity upon stress, providing a positive feedback for the UPR.

The ER-associated degradation (ERAD) is a pathway along which misfolded and unfolded proteins are transported from the ER to the cytosol for proteasomal degradation[103], where they are targeted and degraded by the UPS [80] or via autophagy[102].

Influenza A virus infection and UPR^{ER} inducing

Viruses can exploit the ER to complete some processes of their life cycle[97,107]. IAV use UPR to enhance viral pathogenesis through facilitating folding and trafficking, affecting receptor interaction[108] and modulating host immune responses[109]. Samarasinghe et al. findings' revealed that acute lung injury results from innate sensing of viruses by ER stress, that was found to be responsible for the pathogenicity of pandemic IAV[110].

During productive viral infection, as in the case of IAV, large amounts of viral proteins are synthesized and modified in infected cells, leading to rapid accumulation of viral proteins and disruption of the ER homeostasis. However, if in one way the host mobilizes the UPR in an attempt to restrict virus infection, in another some of UPR major consequences are beneficial to viral replication. Thus, UPR could be a merely a host response or a result of viral manipulation. Both ways, the outcome could be pathogenic[31,33].

According to Goodman et al. results, P58^{IPK} can interact with and inhibit both PKR and PERK, being a critical regulator of both cellular and viral mRNA translation. Yet, they have found that IAV mRNA translation and replication is promoted by P58^{IPK} through PKR inhibition, independently of PERK[112].

Another research conducted by Hassan et al. reported that infection with wild type IAV induces ER stress response in human tracheal and bronchial epithelial cells (HTBECs) through the IRE1 branch, with little or no concomitant activation of the PERK pathway. They also showed that the virus modulates the stress response in the setting of a pre-existing stress by decreasing the activation of the ATF6 pathway. IAV also cause a significant induction of several genes, including CHOP, suggesting ER stress response activation and apoptosis induction[113].

A different approach was reported by Roberson et al. in murine tracheal epithelial cells (MTECs). Their results showed that IAV infection induces ER-stress via ATF6 activation, but not CHOP. They also described that IAV mediated-apoptosis in these cells is caspase-12 dependent, which is another hallmark of ER-stress in infected cells[114].

Recently, chemical genomics identified the PERK pathway as a cellular target for influenza virus inhibition. By screening collections of drugs approved for human use, Landeras-Bueno et al. identified Montelukast (MK) as an inhibitor of virus gene expression and validated these results in virus-infected cells[115]. The authors found that IAV leads to attenuation of the PERK-mediated UPR, but does not downregulates neither ATF6 or IRE1 arms, in contrast to Hassan and Roberson's studies[113,114]. The main difference between approaches was that the latter investigators analyzed UPR activation at very late times after infection (12 to 48h), long after the virus infection cycle is finished (around 8h). In this case[115], the authors show clear down-regulation of PERK phosphorylation as early as 6h after virus infection. This observation is consistent with the activation of $P58^{IPK}$. According to their results, MK induces PERK phosphorylation and counteracts the influenza virus-induced block of the PERK pathway. Therefore, the PERK-mediated UPR was finally considered a potential cellular target for anti-influenza virus treatment, and being a cellular target, it may eventually be useful for inhibiting other fast-replicating RNA viruses.

CHAPTER III

Aims of the study

Human Cytomegalovirus and Innate Immunity

HCMV is widely common in the human population and might be associated with additional long-term health consequences due to its ability to establish a lifelong persistent latent infection. Upon infection, viral components are recognized by intracellular receptors that activate mitochondrial and peroxisomal MAVS-mediated antiviral immune response. This virus encodes an anti-apoptotic protein named vMIA that localizes at mitochondria and peroxisomes, induces their fragmentation and, more importantly, inhibits the cellular antiviral response.

The main goal of this project was to further characterize the role of vMIA in the peroxisome-MAVS dependent antiviral response. To that end, we proposed to study some vMIA sequence-deletion mutants in order to map the protein's domains responsible for peroxisome fragmentation and/or the inhibition of the peroxisome-dependent antiviral response. In order to determine the importance of the peroxisome-dependent antiviral pathway on the control of the HCMV infection, we aimed to use the CRISPR-Cas9 system to create a Pex19 KO cell line where vMia is not able to reach this organelle. We furthermore proposed to analyse the role of the MCMV analogue of vMIA, m38.5, on peroxisomes and the antiviral cellular response, in order to establish whether we could use this virus to complement our studies and be able to perform our analysis in a (cellular or animal) infection context.

Influenza A Virus and Quality Control Machinery

IAV been the causative agent for most of the annual epidemic in humans and the major pandemics of influenza in the last century. Previous studies have shown that, during infection, it occurs the accumulation of unfolded proteins within the ER and the formation of specialized sites of viral replication, resulting in the formation of insoluble aggregates or inclusions. It is known that IAV modulates UPR ER stress-induced and uses the aggresome processing machinery for host cell entry, specifically during uncoating.

In this study we proposed to determine whether IAV infection leads to aggresomal-prone proteins accumulation, throughout the immunostaining detection of aggresomes or protein aggregates; characterization of the insoluble protein fraction within the cells over time; and the analysis of the activation of the UPR pathway.

CHAPTER IV

Materials and Methods

4.1 Materials

4.1.1 Cell lines

HeLa	Human cervix adenocarcinoma cells; stable cell line expressing the fluorescent reporter HSP27-GFP
Mef MAVS-PEX	Mouse Embryonic Fibroblasts with MAVS only at peroxisomes
A549	Human alveolar basal epithelial adenocarcinoma cells
HFF	Human foreskin fibroblasts
293T	Human embryonic kidney cells

4.1.2 Cell Culture Solutions

Dulbecco’s Modified Eagle Medium (DMEM) High Glucose w/ L-Glutamine w/o Sodium Pyruvate, Gibco

Fetal Bovine Serum (FBS), qualified, E.U.-approved, South America origin, Gibco

Penicillin/Streptomycin, Gibco

Dulbecco's Phosphate Buffered Saline w/o Calcium w/o Magnesium, Gibco

Trypsin-EDTA 1X in PBS w/o Calcium w/o Magnesium w/o Phenol Red, Gibco

Opti-MEM Reduced-Serum Medium (1x), Gibco

4.1.3 Bacterial strains

Escherichia coli	DH5α

4.1.4 Bacterial Media

LB/Agar:	2g Agar, Formedium 20 g Lysogeny broth (LB), Fisher Scientific 1 L ddH2O

Antibiotics	Ampicillin (Amp), Sigma-Aldrich
	Kanamycin (Kan), Sigma-Aldrich

4.1.5 Viruses

Influenza A virus

PR8	Influenza virus strain A/Puerto Rico/8/1934 (H1N1)
△NS1	Influenza PR8 virus that lacks NS1 protein

4.1.6 Plasmids

Gene	**Tag**	**Antibiotic Resistance**
RIG-I-CARD	GFP	Kan
vMiaΔ131-147	Myc	Amp
vMiaΔ115-130	Myc	Amp
vMiaΔ23-34	Myc	Amp
vMiaΔ2-23	Myc	Amp
m38.5	HA	

4.1.7 Vectors

Transfer pSicoR-CRISPR-Cas9 guideRNA lentiviral vector (RP-418)

Packaging vector pCMV R8.81

Envelope vector pMD2.G

4.1.8 Primers and Oligonucleotides

PCR primers	Manufacture: Eurofins.	
IRF1	IRF 1 mouse	forward 5’ GGTCAGGACTTGGATATGGAA 3’
		reverse 5’ AGTGGTGCTATCTGGTATAATGT 3’
GAPDH		
	GAPDH mouse	forward 5’ AGTATGTCGTGGAGTCTA 3’
		reverse 5’ CAATCTTGAGTGAGTTGTC 3’

Oligonucleotides for CRISPR/Cas9 system			
PEX19	Oligo I	forward 5’ **AAC**GCAAGTCGGAGGTAGCAAGA 3’	
		reverse 5’ **AAAC**TCTTGCTACCTCCGACTTG 3’	
	Oligo II	forward 5’ **AAC**GCTGAGGAAGGCTGTAGTGT 3’	
		reverse 5’ **AAAC**ACACTACAGCCTTCCTCAG 3’	
	Oligo III	forward 5’ **AAC**GTGTCGGGGCCGAAGCGGAC 3’	
		reverse 5’ **AAAC**GTCCGCTTCGGCCCCGACA 3’	

4.1.9 Transfection Reagents

Lipofectamine® 3000 Transfection Reagent, Invitrogen

Polyethylenimine (PEI)

4.1.10 Markers and Loading Dyes

GRS Protein Marker Multicolour Tris-Glicine 4~20%, Grisp

6x Laemmli Buffer with DTT and Bromophenol Blue

O' Gene Ruler DNA Ladder Mix, Thermo Fisher

6x Orange DNA Loading Dye, Thermo Fisher

4.1.11 Enzymes

Restriction endonucleases	**Restriction site**	**Buffer**
BsmBI (Esp3I)	5’CGTCTC(N)1|3’ 3’GCAGAG(N)5|5	10x Fast Digest Buffer, Thermo Fisher Scientifics

T4 DNA ligase	10x T4 DNA ligase Reaction Buffer, New England’s Biolab
M-MuLV reverse transcriptase	10x M-MuLV Reverse Transcriptase Buffer, New England’s BioLab

4.1.12 Kits

NucleoBond® Xtra Midi, Macherey-Nagel

Pierce™ Bovine Serum Albumin (BCA) Protein Assay Kit, Thermo Scientific

Proteostat Aggresome Detection Kit, Enzo

Protran BA85 Nitrocellulose Blotting Membrane, GE Healthcare

4.1.13 Antibodies

Primary	Species	Production	Dilution		Company
			IMF	WB	
PMP70	Mouse	Monoclonal	1:200	-	Sigma-Aldrich
HA	Rat	Monoclonal	1:1000	-	
Myc	Rabbit	Monoclonal	1:100	-	Cell Signaling
PEX19	Mouse	Monoclonal	-	1:50	Sigma-Aldrich
Anti-ATF6 (α)	Mouse	Monoclonal	-	1:400	Stressgen
Tubulin	Mouse	Monoclonal	-	1:4000	Sigma-Aldrich
Actin	Mouse	Monoclonal	-		

Secondary	Species	Production	Dilution		Company
			IMF	WB	
Alexa 488	Rabbit	Polyclonal IgG (H+L)	1:500	-	Invitrogen-Molecular Probles
	Mouse		1:400	-	
Alexa 647	Mouse		1:500	-	
TRITC	Rabbit		1:200	-	
	Mouse		1:100	-	Jackson Imunoresearch
HoechstDye	-	-	1:200	-	
IRDye®680CW	Mouse	Polyclonal	-	1:10000	LI-COR
IRDye®800CW	Rabbit	IgG (H+L)	-	1:1000	LI-COR

4.1.14 Solutions and Buffers

Blotting Buffer:	0,05 M Tris, 0,4 M Glycine, 0,05% SDS, 20% Methanol
BSA 1%:	2% BSA diluted in 1x PBS
ELB	0.5% Triton X-100, 50mM Hepes pH7, 250mM NaCl, 1mM DTT, 1mM Naf, 2mM EDTA, 1μM EGTA, 1mM Na_3VO_4 in ddH_2O Add protease inhibitors before use: 0,01 mM Foy, 0,25 (v/v) Trasylol, 0,1 mM PMSF
Loading buffer:	1 M Tris pH 6.80, 10% Glycerol, 1 M DTT, 20% SDS, β-Mercaptoethanol, 0,1% Bromophenol Blue

Milk for Blot blocking:	5 g of powder milk in 100 mL of 1x TBS-T
Mounting Medium:	N-propyl-Gallat: 2.5% (w/v) n-propyl-gallat; 50% glycerol, in PBS Mowiol: 12 g Mowiol 4-88, 20 mL Glycerol, 40 mL PBS Mounting medium: 3:1 mixture Mowiol with n-propyl-gallate
1x PBS:	1,37 M NaCl, 80 mM NaHPO4, 0,0268 M KCl, 0,0147 M KH2PO4 pH 7,34, prepared from 10x PBS diluted in ddH2O
PFA 4 %:	20 g PFA in 450 mL ddH2O, 4 drops 1 M NaOH, 50 mL 10x PBS
Running Buffer 1x:	250 mM Tris, 1,9 M Glycine, 1% SDS
1x TAE:	0.04 M Tris, 0.02 M Acetic Acid, 1 mM EDTA pH 8, prepared from TAE 50x diluted in ddH2O
TBS-T:	1X TBS-T (100 mM Tris Base, 150 mM sodium chloride and 0,05% Tween-20 [pH 8])
0,2%Triton X-100:	0.2% Triton X-100 in 1x PBS

4.1.15 Databases and Software

Axio Imager Software, Zeiss

DeNovix DS-11 Software, DeNovix

Excel, Microsoft

Graphpad, Prism 7

Image Lab, Bio-Rad

Image Studio Software for Odyssey

National Center for Biotechnology Information (NCBI)

Quantity One 1-D Analysis Software, Bio-Rad

Zen Software, Black Edition, Zeiss

4.2 Methods

4.2.1 Cell Culture

Cell Lines Maintenance

Mef MAVS-PEX cells and HeLa HSPB1-GFP were kindly provided by Dr. Kagan from Harvard Medical School and Dr. Ana Soares from iBiMED, respectively. Both cell strains, along with 293T and HFF cells, were routinely cultured and split twice a week in 10øcm culture dishes with DMEM high glucose (4,5 g/L) (Gibco ©, Life Technologies, Germany) supplemented with 10% FBS and 1% (100U/mL) of penicillin and streptomycin, termed as complete DMEM. The cells were maintained in culture at 37°C in a humidified atmosphere containing 5% CO2.

Confluent cells were washed with PBS and after incubating with 1.5 mL trypsin-EDTA at 37°C and 5% CO_2. When individual cells separated and detached from the dish surface, cells were resuspended in culture medium, centrifuged at 1000 *g* for 3 minutes at room temperature and either divided according to experimental needs and/or seeded in a 1:10 dilution (≈105 cells/mL).

Cell storage, freezing and thawing

Cells stocks were prepared from confluent cells resuspended in freezing medium (DMEM supplemented with 10% FBS and 10% DMSO) and were kept in cryovials aliquots of 1mL. Stocks were frozen in -80°C before being placed in the liquid nitrogen tank for cryopreservation.

When needed, frozen cells were thawed through resuspension with pre-warmed culture medium and seeded in a 10øcm culture dishes. After cell adhesion (≈ 5 hours) the medium was replaced by fresh growth medium to remove cell debris and DMSO.

4.2.2 Transformation of competent bacteria

Heat shock transformation

For bacterial transformation, 1 µL of ligation DNA were added to 45 µL of competent *Escherichia coli* DH5α cells, gently mixed and incubated for 30 minutes on ice. Heat shock was performed by exposing bacteria at 42°C for 90 seconds followed by a short incubation on ice, allowing the DNA to be incorporated. After, bacteria recuperated in 750 µL of LB for 45 minutes at 37°C 180 *g*. Bacterial suspension was centrifuged for 1 minute at 1700 *g* and most supernatant was discarded. The pellet was resuspended in the remaining supernatant and glass beads helped to spread bacteria in LB/agar plates complemented with the appropriate antibiotic, which were incubated at 37°C overnight. The protocol was done under a sterile environment and the appropriate controls were used.

This method was used to obtain midi-preps from vMIA Δ131-147, vMIA Δ23-34 and vMIA Δ2-23.

Colonies were picked and inoculated in 3 mL of LB medium with antibiotic for 16 hours at 37°C with shaking 180 *g*. Cell suspension were then grown in 200 mL of LB medium with antibiotic overnight under the same conditions. Plasmids were purified following the NucleoBond® Xtra Midi (Macherey-Nagel) protocol.

Electroporation

Prior to electroporation, 50 µl of competent *E. coli* were mixed with 3 µl of the plasmid to be transformed. The mixture is transferred into a chilled plastic or glass 2 mm cuvette which has two aluminum electrodes on its sides, ensuring a direct contact between the electrodes and the suspension. Electroporation was performed with a 2.5 kV pulse appliance which create an electrostatic field in a cell solution. Immediately after, one mL of LB was added to the suspension and it was transferred back into the Eppendorf tube, followed by an incubation at 37°C, the bacteria optimal temperature for at least an hour to allow recovery of the cells and expression of the plasmid. The suspension was then centrifuged at 700 g for 90 seconds, and most supernatant was discarded. The pellet was resuspended in the remaining supernatant the bacteria was plated in LB/agar plates complemented with the appropriate antibiotic, which were incubated at 37°C overnight. The protocol was done under a sterile environment and the appropriate controls were used.

Several colonies were picked and inoculated in 5 mL of LB medium with antibiotic overnight 37°C with shaking 180 *g*. Plasmid isolation was accomplished through a miniprep protocol. 2 mL of each bacterial suspension was centrifuged at 6000 *g* for 5 minutes. The pellet was resuspended in 300 µl of solution I and lysed with 300 µl of solution II, mixed and incubated 5 minutes at room temperature before being neutralized with 300 µl of solution III. Then, it was centrifuged at 16 200 *g* at 4°C and the supernatant was kept and mixed with 600 µl of isopropanol. The centrifugation was repeated and the pellet was kept and resuspended in 600 µl of 70% ethanol. Once again, the centrifugation was repeated and the pellet resuspended in TE buffer with the appropriate volume and store it at 4°C.

Midiprep with the NucleoBond® Xtra Midi

High-copy plasmids were extracted from 200 ml bacterial cultures, which were inoculated with a single bacterial clone in LB medium with the appropriate antibiotic and grown overnight at 37°C and 800 rpm. When the optical density reached between 0.2-0.4, bacterial cells were pelleted by centrifugation at 6000g for 15 minutes at 4°C, and supernatants were discarded. Bacterial cells were completely resuspended, lysed, neutralized and centrifuged. Plasmids were then purified following the NucleoBond® Xtra Midi (Macherey-Nagel) protocol and the concentration of extracted DNA samples was analyzed with Nanodrop (DeNovix).

4.2.3 Transient Mammalian Cell Transfection Methods

Lipofectamine 3000

Lipofectamine™ 3000 Reagent Protocol (Invitrogen) was followed according to the manufacturer. To prepare plasmid DNA-lipid complexes, the transfectable DNA together with P3000 reagent (1:1 ratio) was added to Lipofectamine 3000 reagent both diluted in OptiMEM and incubated for 5 minutes at room temperature. The complex formed was then added dropwise to 6-well plates to a final volume of 2 mL and it was incubated under growth conditions for 6 hours or 24 hours. This method was used to transfect Mefs MAVS-PEX cells with different quantities of DNA (2.7 µg of GFP-RIG-I-CARD, and 3.5 µg vMIA mutants/m38.5).

Polyethylenimine (PEI)

To perform transfection with PEI in 6-well plate, 10 µg plasmid of DNA was diluted in 500 µl of serum-free DMEM (MOA) and PEI (1 µg/µl) was added to the diluted DNA. The volume of PEI used is based on an 8:1 ratio of PEI (µg): total DNA (µg). After mixed, the solution was incubated during 20 minutes at room temperature and added to the cells in a dropwise manner. PEI condenses DNA into positively charged particles that bind to anionic cell surfaces, the DNA:PEI complex is endocytosed by the cells and the DNA released into the cytoplasm. The medium was changed to complete DMEM six hours post-transfection.

This procedure was performed to transfect 293T cells with 4 µg of CRISPR-Cas (418), 1 µg of pCMV R8.81 and 3 µg of pMD2.G vectors, using 32 µl of PEI. All steps were carried out using sterile techniques in a laminar flow hood.

4.2.4 Immunocytochemistry

Immunofluorescence

Cells grown in **12ømm** glass coverslips were washed three times with PBS before being fixated for 20 minutes with 4% PFA solution, permeabilized with 0,2% Triton X-100 for 10 minutes and blocked with 1% BSA for 10 minutes, all procedures being performed at room temperatures. After, cells were stained with 20 µL of the primary antibody for 1 hour and with the secondary antibody for 1 hour in a humid environment, protected from the light. In some cases, the staining with Proteostat Aggresome Dectetion kit (Enzo Life Sciences International) was performed, according with the manufacturer's instructions. When needed, cells were incubated with 30 µL of Hoechst dye for 2 minutes. All the incubations were done at room temperature and between each step the cells were washed three times with PBS. Coverslips were washed in ddH2O, mounted in glass slides with mounting medium (Mowiol) and dried for at least 24 hours. Glass slides were stored at 4°C until observation under a fluorescence or a confocal microscope.

The cells were observed with AxioImager Z1 Zeiss Microscope and AxioVision Software, using 100x/1.40 oil objective equipped with the appropriate filter combination. Confocal photos were acquired and further analyzed with a Zeiss confocal microscope, using 100x/1.40 oil objectives and Zeiss Black Edition Software. The lasers used were 488 nm Argon-ion laser, 561 nm DPSS laser and 642 nm HeNe for samples stained with Alexa Fluor 488 dye/GFP, TRITC/Proteostat dye and Alexa 647 dyed, respectively.

4.2.5 Reverse transcriptase - quantitative Polymerase Chain Reaction (PCR)

RNA extraction

Cells in 6-well plate were washed with PBS and lysed at room temperature with 500 µL of Trifast/Trizol. After being harvested by pipeting up and down, the samples can be stored at -80º C. If so, in order to proceed, samples should be thawed and incubated for 5 minutes at room temperature.

To obtain a fractionated solution of cellular content, 100 µL of chloroform were added, the samples were shaken vigorously for 15 seconds and incubated for 5 minutes at room temperature. Following a centrifugation of 15 minutes at 12000 *g*, the upper aqueous phase containing RNA was extracted. RNA was incubated on ice with 250 µL of isopropanol for 10 minutes. After centrifugation for 15 minutes at 12000 *g*, the supernatant was removed and the pellet was washed two times with 500 µL of 75% ethanol interspersed by maximum speed centrifugation at 4ºC for 5 minutes. After removing the ethanol, the pellet dried for 10 minutes, was resuspended with 20 µL of RNAse free water and dissolved at 55°C. The RNA concentration was measured with the Nanodrop (DeNovix) equipment.

cDNA synthesis

cDNA synthesis was accomplished by mixing 1µg RNA with a master mix of 280 pmol oligo-dT primer, 166 µM dNTPs, 1x M-MuL V Reverse transcriptase buffer, 100 U M-MuL V Reverse transcriptase, 20 U RNAse inhibitor and RNAse free water. This mixture was incubated for 10 minutes at room temperature and, afterwards, cDNA was via reverse transcription (Figure 12). At this point cDNA can be stored at -30°C.

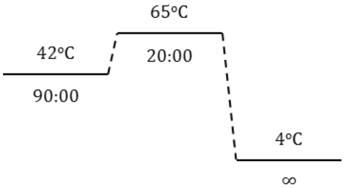

Figure 12 Reverse transcription PCR cycle of cDNA synthesis. cDNA was synthesized for 90 minutes at 42°C and the enzyme was inactivated for 20 minutes at 65°C

Polymerase chain reaction and DNA electrophoresis

To check cDNA integrity, it should be analyzed by PCR (Figure 13) using primers designed to the intronic sequences of a standard, constitutively expressed housekeeping gene, and gel electrophoresis. 2 µl of each cDNA was used as template in the PCR reaction, together with 170 nM mouse GAPDH primers, 166 µM dNTPs, 1x Reaction Buffer NZYTaq DNA Polymerase, 1,41 mM $MgCl_2$, 2,5 U NZYTaq DNA Polymerase and Nuclease-free water.

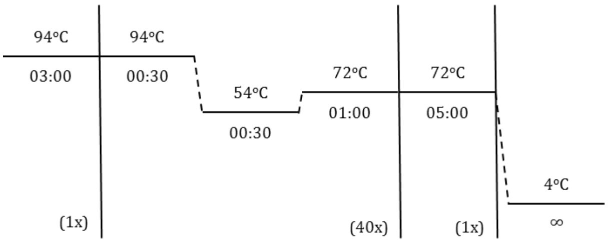

Figure 13 PCR cycle used to amplify GAPDH gene. The PCR started with an initial denaturation step for 3 minutes at 94°C, followed by 40 cycles of a denaturation-annealing-extension step, and a last final extension that last for 5 minutes at 72°C.

PCR products ran by DNA electrophoresis in a 1% agarose gel in 1x TAE. After the molten gel had partially cooled, Midori Green DNA Stain was added and the gel was poured into gel trays. Completely set and hardened gels were mounted into electrophoresis chambers and covered with TAE buffer. Samples for analysis were mixed with 1x Orange DNA Loading Dye (ThermoFisher) and loaded into the sample wells. Electrophoresis was carried out at 100 V for 40 minutes in 1x TAE running buffer, using O'GeneRuler DNA Ladder Mix (Thermo Fisher) to allow sizing and quantification. DNA in the gel was visualized and digital images were obtain using GelDoc (BioRad).

Real-time Quantitative Polymerase Chain Reaction

The primer sequences used for quantification of **mouse IRF1** were fwd 5' **GGTCAGGACTTGGATATGGAA** 3' and rev 5' **AGTGGTGCTATCTGGTATAATGT** and for **mouse GAPDH** were fwd 5' **GCC TTC CGT GTT CCT ACC** 3' and rev 5' **CCT GCT TCA CCA CCT TCT T** 3'. All were previously described by Magalhães et al[31].

The real-time polymerase chain reaction mix was prepared with 2 µL of 1:10 diluted synthesized cDNA, 10 µL of 2× iTaq SYBR Green Master Mix (BioRad) and each primer was added to a final concentration of 250 nM for a total volume of 20 µL. The fluorescence was measured after the extension step (Figure 14), using the7500 Real-Time PCR System and its software (Applied Biosystems). After the thermocycling reaction, the melting step was performed with continuous measurement of fluorescence.

Data analysis was performed using the $2^{-\Delta\Delta CT}$ method.

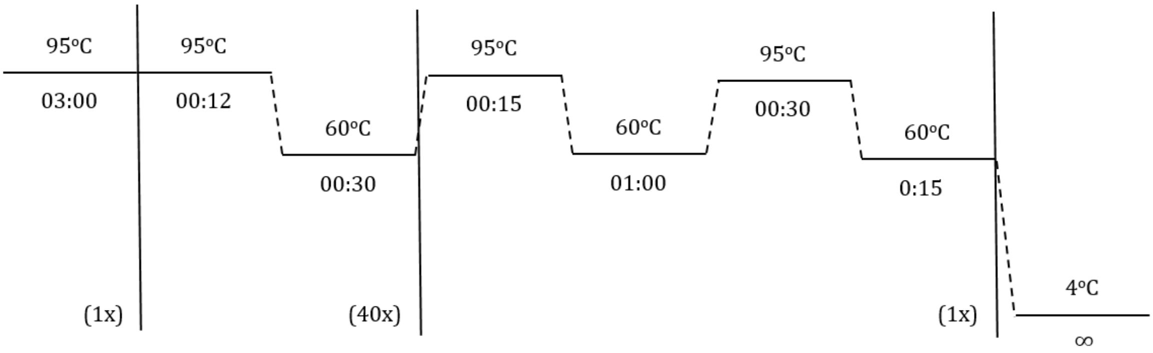

Figure 14 RT-qPCR cycling protocol. The reaction initiated by heating at 95°C for 3 min, followed by 40 cycles of a 12 seconds denaturation step at 95°C and a 30 seconds annealing/elongation step at 60°C. After the thermocycling reaction, the melting step was performed with continuous measurement of fluorescence

4.2.6 Infection

To perform infection with IAV, HSPB1-GFP HeLa and A549 cells were seeded witha density of 2x10^5 cells (day 0) for protein extraction protocol and 2.4x10^4 cells for immunofluorescence experiments, taking in consideration that both cell lines duplicate in 24 hours.

The day after, cells were washed with Serum Free Media (SFM) [DMEM supplemented with Pen-Strep and Glutamine – without FBS because its inhibits virus entry] and infected with Influenza A virus PR8 (4x10^7 pfu/ml) and the ΔNS1 mutant strain (that lacks the NS1 protein) (4.7x10^7 pfu/ml) at a MOI of 3, prepared in SFM. After, the plates are incubated for 5 minutes, mixing at room temperature, followed by a 35 minutes incubation at 37°C in 5% CO_2. Complete media was then added (to stop the viruses to continue entering the cell) and the plates were again incubated for the desired times at 37°C in 5% CO_2.

4.2.7 Immunobloting

Lysis and harvesting – total protein extraction and quantification

After infection, cells were washed 1x with PBS and harvested with 500 μL of Empigen Lysis Buffer (ELB) suplemented with inhibitors per well (up&down). Samples were centrifuged for 20 minutes at 200 *g* at 4°C. The supernatants were kept and total protein was quantified (can be stored at -20°C). During all procedures, cells remained on ice to avoid the activity of proteases.

Insoluble protein fraction

To isolate the insoluble protein fraction, the volume corresponding to 100μg of total protein was diluted in 80 μL of ELB and 20 μL of NP40 (10%). Samples were sonicated for 20 seconds (three times). After sonication cycles, samples undergone another centrifugation (16,000 *g*, 20 minutes at 4 °C). The supernatant was removed, the pellet was solubilized with 50μL of ELB.

Protein Sodium Dodecyl Sulfate-Polyacrylamide Gel Electrophoresis (SDS-PAGE)

Desired concentrations (μg) of protein extracts were diluted in 5x loading buffer (DTT and bromophenol blue) and denatured for 5 minutes at 95°C. After, samples were loaded alongside with a pre-stained protein marker (GRS Protein Marker Multicolour Tris-Glicine 4~20%, Grisp) in mini handcast gels prepared with 10-12% polyacrylamide resolving gel and 4% stacking gel. The electrophoretic chamber was filled with 1x concentrated Running Buffer and the electrophoresis was conducted for 2 hours, first at 80 V to allow the samples to pass through the stacking gel, and then at 110 V. Bromophenol blue presented in the loading buffer allowed sample running visualization.

Gels obtained for total/insoluble protocol were stained with BlueSafe, according to the manufacturer's instruction and the results were observed using the Odyssey scanner and its software (LI-COR, Biosciences, US).

Western Blot and Immunodetection

After protein's separation, proteins were electro transferred onto a nitrocellulose membrane in the Trans-Blot® Turbo™ Transfer System for at 25 V, 0,4 A for 7 minutes.

The membranes were washed three times, 5 minutes each, with 1x tris-saline buffer with tween 20 (TBS-T) to take out the methanol residues and were blocked using 5% (w/w) low fat powder milk or 2% Bovine Serum Albumin (BSA) diluted in TBS-T for 1 hour at room temperature. Membrane staining was accomplished by incubation with primary antibodies at room temperature for 1 hour or at 4°C overnight, and the respective secondary antibodies during 1 hour at room temperature protected from light, under agitation. Between incubations, three washing steps of 5 minutes each with TBS-T were performed.

Digital pictures of the stained membranes were obtained in the Odyssey scanner and analyzed in its software (LI-COR, Biosciences, US), using tubulin intensity as normalizer. The Odyssey system is equipped with two infrared channels for direct fluorescence detection on membranes at 700 and 800 nm.

4.2.8 Quantification methods

Nucleic Acids quantification

DNA and RNA quantification was performed using DeNovix. Since both nucleotides absorb at 260 nm, purification of the samples is required prior to measurement. The photometer measures simultaneously the absorbance at 230, 260 and 280 and displays A260/A280 and A260/A230 ratios determining the contamination of the samples with protein specimens and organic compounds, respectively. The generally accepted 260/280 values are around 1.8 for pure DNA and 2.0 for RNA, while the 260/230 values for nucleic acids usually range between 1.8 and 2.2.

Bovine Serum Albumin Protein Assay

Pierce™ Bovine Serum Albumin (BCA) Protein Assay Kit (Thermo Scientific) was performed to quantify total protein following the manufacturer´s instructions. The total extracts were incubated with the BCA reagent for 30 minutes at 37 °C, followed by absorbance measurement at 575 nm in a microplate reader.

4.2.9 Clustered Regularly Interspaced Short Palindromic Repeats/CRISPR associated system 9 (CRISPR/Cas9) for gene knockout

Restriction digestion and Ligation

Lentiviral CRISPR-Cas9 constructs were generated by cloning double-strand oligonucleotide **inserts** into a pSicoR-CRISPR-Cas9 lentiviral vector (RP418), puromycin resistance.

RP418 vector was digested with BsmBI (Esp3I) Fast Digest restriction enzyme (together with 1x Fast Digest Buffer and 1 mM DTT) at 37ºC for 30 minutes. Digested samples ran on 1% agarose gel in 1x concentrated TAE buffer at 120 V for 1 hour in 1x TAE running buffer. The bands of interest were excised under the UV light with a scalpel, followed by isolation and purification with NucleoSpin® Gel and PCR clean-up (Macherey-Nagel) as the protocol indicates.

The Oligo-gRNA of interest were previously designed. After reconstruction, 10 µM of each primer were mixed together and annealed as the mixture was heated up to 95ºC for 5 minutes and 10 minutes on ice. At this point, oligo-gRNA can be stored at 4ºC for later usage.

The ligation was performed using 10 ng of the linearized vector and 10 µl of gRNA and both were incubated with a T4 DNA ligase in NEBuffer U at 16°C overnight. The resulting plasmid was used to transform bacteria according to the electroporation protocol described before.

Transfection and transduction (Retroviral infection of cells)

Lentiviral RP418—OligoRNA constructs were transfected together with envelope and packaging plasmids, pCMV R8.81 and pMD2.G, into 293T cells for lentivirus production. 293T cells were seeded in a 10øcm plate with a density of $3x10^6$ cells per plate. Transfection was performed using PEI, as previously described.

HFF cells were seeded in 6-well plates with a density of $0.75x10^5$ cells, using 3 wells per condition. To perform transduction, the virus supernatant was filtered through a __ cm syringe. 5µ of polybrene was added to the medium and 3 mL were added to the cells. Centrifugal enhancement was performed at 2300 rpm for 30 minutes. The medium was replaced 24 hours after the retroviral infection and cells were cultured for 48 hours. Plate the cells from each oligo-gRNA into 10 cm plate.

Cells selection

Growth medium was replaced with selective medium containing puromycin using a final concentration of 2µg/ml. Selection medium was replaced with normal growth medium after mock infected cells showed no survivors. Transduced cells were expanded and further characterized by Western Blot analysis. Additionally, single sell selection was performed according to Cell Cloning by Serial Dilution in 96-well plates Protocol (Corning) and the clones were also characterized.

4.2.10 Statistical Analysis

Statistical analysis was achieved using Graph Pad Prism 7. Data were attained for the quantitative analysis of IRF1 mRNA from three independent experiments and represent the means ± standard error mean (SEM). To determine the statistical significance between the experimental groups the one-way ANOVA followed by Bonferroni's multiple comparison tests were applied. P values of ≤ 0.05 were considered as significant.

CHAPTER V

Results and Discussion

5.1 Human Cytomegalovirus and Innate Immunity

Upon infection, intracellular RLR recognize viral components and activate a MAVS-mediated antiviral immune response, that culminates with the production of type I IFN and of pro-inflammatory cytokines. MAVS has been shown to localize at mitochondria[32] and peroxisomes[33], both comprising specific and complementary antiviral responses, although temporally and functionally different[20,29]. HCMV's protein vMia is known to block apoptotic signaling pathways and subvert the mitochondria and peroxisome-dependent host antiviral response[31,41,54].

Castanier et al[54] reported that RLR activation promotes elongation of the mitochondrial networks, and further suggested that mitochondria elongation induces MAVS-mediated signaling, whereas its fragmentation has the opposite effect. Furthermore, the authors showed that vMIA promotes mitochondrial fragmentation and consequently impedes downstream MAVS signalling[54]. Our group has previously demontrated that vMIA travels to peroxisomes via interaction with the Pex19 chaperone, where it interacts with MAVS and induces peroxisomes' fragmentation[30]. However, this organelle morphology change is not essential for the role of vMIA on the evasion of the immune response[30]. Hence, both reports point towards two distinct mechanisms relating organelle's fragmentation and its interplay with the inhibition of the antiviral response.

In order to unravel these specific mechanisms, we proposed to analyze several vMIA mutants who lack different amino acid sequences, in order to map the domains responsible for either peroxisomal fragmentation or MAVS-dependent immune response.

Mapping the vMIA domains responsible for organelles' morphology change

Goldmacher et al[41] first characterized the amino-terminal 2–23 amino acid sequence of vMIA as necessary for both anti-apoptotic activity and mitochondrial targeting. A mutant lacking the 2-23 sequence abrogated vMIA anti-apoptotic function and evidently altered its staining pattern to cytoplasm, as it is neither evidently translocated to the ER nor into mito[45].

Further studies[44,46,116] identified two necessary and sufficient domains required for its antiapoptotic activity, namely 5-34 and 118-147. Hayajneh et al[44] showed that a mini vMIA Δ35-112/Δ148-163, consisting essentially of just the two functional domains, retained antiapoptotic function; and moreover demonstrated that the mitochondrial localization signal is located within the 2-30 segment of vMIA.

It is also known that vMIA inhibits apoptosis by binding and sequestering Bax at mitochondria[46,116], demonstrating that there is a strong correlation between the anti-apoptotic function of vMIA and its ability to bind and relocate Bax.

The characteristics of some of the vMIA mutants used in the studies mentioned above are represented and summarized in Figure 15.

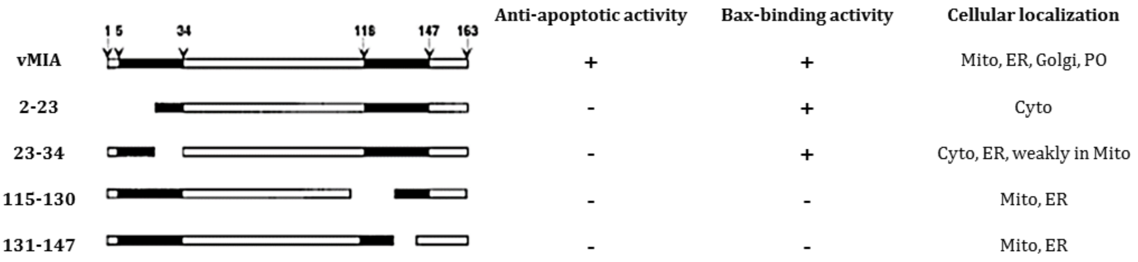

	Anti-apoptotic activity	Bax-binding activity	Cellular localization
vMIA	+	+	Mito, ER, Golgi, PO
2-23	-	+	Cyto
23-34	-	+	Cyto, ER, weakly in Mito
115-130	-	-	Mito, ER
131-147	-	-	Mito, ER

Figure 15 Structural and functional characterization of vMIA and different sequence-deletion vMIA mutants. Several studies have defined two essential and sufficient anti-apoptotic domains (in black) in vMIA, with either a mitochondrial localization signal or bax-binding activity.

To determine whether these mutants co-localize with peroxisomes and analyse their possible effect on the organelle's morphology, their myc-tagged constructs were transfected into Mef cells that express MAVS solely at peroxisomes (MAVS PEX cells)[33]. After 24h, these cells were subjected to immunolocalization analyses with antibodies against Myc and PMP70 to stain the vMIA mutants and peroxisomes, respectively.

The obtained results (Figure 16 B) show that all the tested mutants co-localize with peroxisomes. In order to analyse the effect of these mutants on peroxisome morphology we compared the size and shape of the organelles with the ones presented in the control untransfected MAVS-PEX cells (Figure 16 A a). where most peroxisomes assume an elongated or rod-shape. Hence, in this study we considered the cells containing "fragmented peroxisomes" as those whose peroxisomes were significantly smaller and in higher number when compared to the control cells.

Upon overexpression of the Δ23-34 mutant, one can observe an apparent mitochondria and peroxisome fragmentation. This peroxisomal morphology change is not observed upon overexpression of the Δ115-130 mutant, (consistently to what is observed for mitochondria). On the other hand, the Δ131-147 mutant seems to somehow affect peroxisome morphology as peroxisomes appear rounder, larger and in higher number when compared to control cells. To note also that a higher degree of co-localization with this organelle is observed for this mutant in comparison with the other two and wild-type vMia. Whether this morphology change reflects a peroxisomal proliferation remains to be investigate.

Previous studies have shown that only the Δ115-130 and Δ131-147 mutants co-localize with mitochondria[44,45]. Although we have not yet performed analyses with mitochondrial markers, in our study all the three mutants seem to assume a typical mitochondrial localization pattern. Δ115-130 seems to have no effect on mitochondria morphology and both Δ23-34 and Δ131-147 seem to induce organelle's fragmentation. The results obtained for the Δ23-34 mutant seem to contradict the localization pattern that has been previously shown[41]. Naturally, these results have to be confirmed with quantification studies using mitochondrial markers. Nevertheless, and similarly to peroxisomes, the Δ115-130 domain seems to be necessary for the organelle's fragmentation.

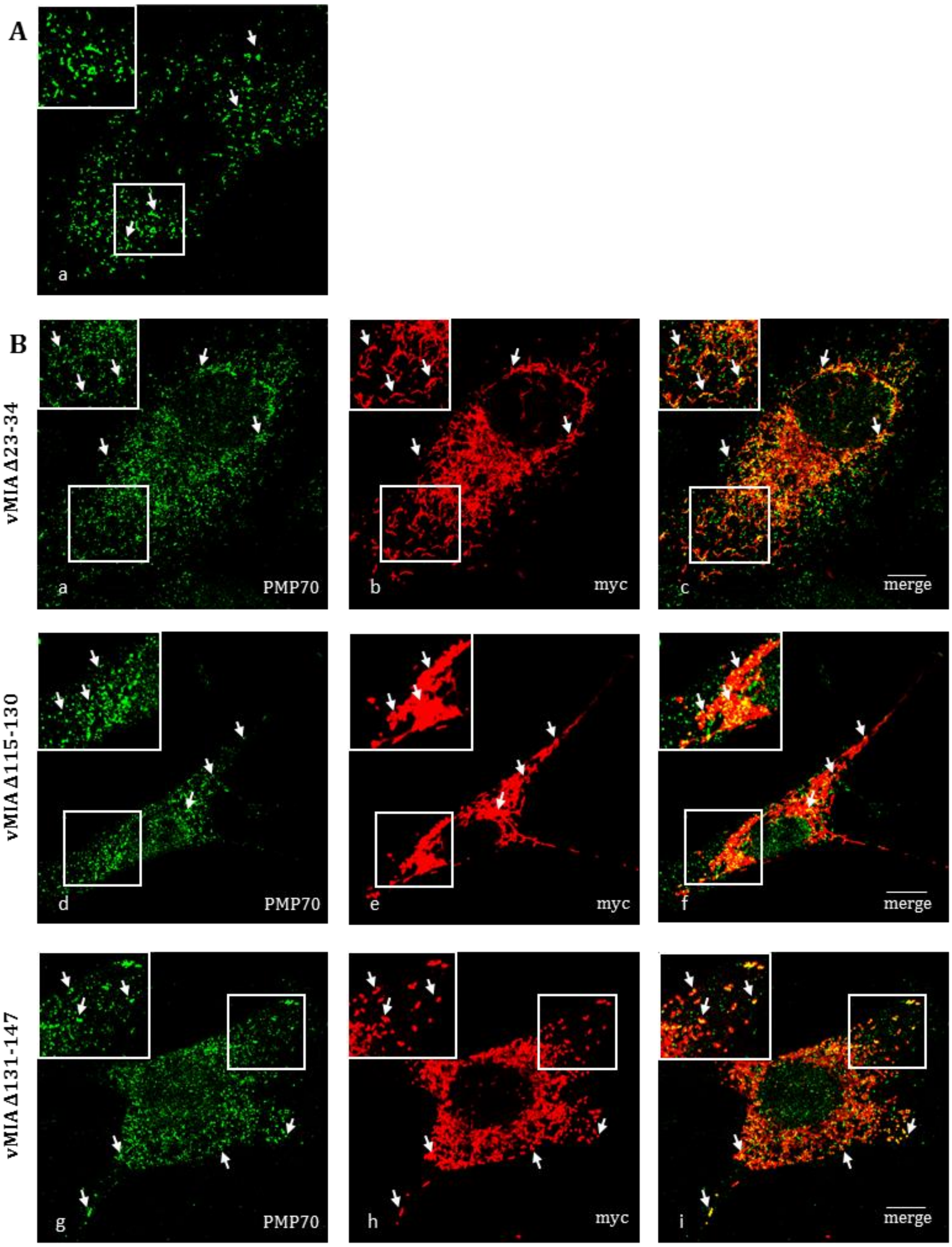
A
a
B
vMIA Δ23-34
a
PMP70
b
myc
c
merge
vMIA Δ115-130
d
PMP70
e
myc
f
merge
vMIA Δ131-147
g
PMP70
h
myc
i
merge

Figure 16 Peroxisomal morphology and vMIA mutants localization in MAVS PEX cells. Confocal images from immunofluorescence staining of peroxisomes and vMIA mutants with PMP70 and myc, respectively. (A a) untransfected MAVS-PEX cells [31] (B) cells transfected with vMIA (a-c) Δ23-34, (d-f) Δ115-130 and (g-i) Δ131-147. Bars correspond to 10μm. Arrows indicate co-localization loci between Myc-vMIA mutants and peroxisomes.

These results seem to indicate than none of the deleted domains has affected the localization of the protein at peroxisomes. Importantly, the 115-130 domain seems to be necessary for the organelle's fragmentation to take place. However, in this study only a few cells (10-20 in each case) were analysed. A quantitative analysis of a higher number of cells (currently being performed) is obviously needed to obtain a solid conclusion.

Mapping the vMIA domains responsible for the inhibition of innate immune response

The peroxisomal MAVS-dependent antiviral pathway is responsible for the early induction of ISGs such as IRF1[33]. To study the effect of the previously mentioned vMIA mutants on the inhibition of the peroxisomal antiviral response, they were overexpressed in MAVS-PEX cells and IRF1 mRNA production was quantified by RT-qPCR. Twenty-four hours after the transfection of the mutants, the cellular antiviral response was stimulated by overexpressing a constitutively active version of RIG-I, RIG-I-CARD[31,117], composed solely by the CARD domains of RIG-I and allowing their direct exposition to MAVS without needing an activator ligand for RIG-I, hence mimicking a viral infection.

As shown in Figure 17, the presence of all three vMia mutants resulted in the inhibition of the IRF1 mRNA production induced by the presence of RIG-I-CARD.

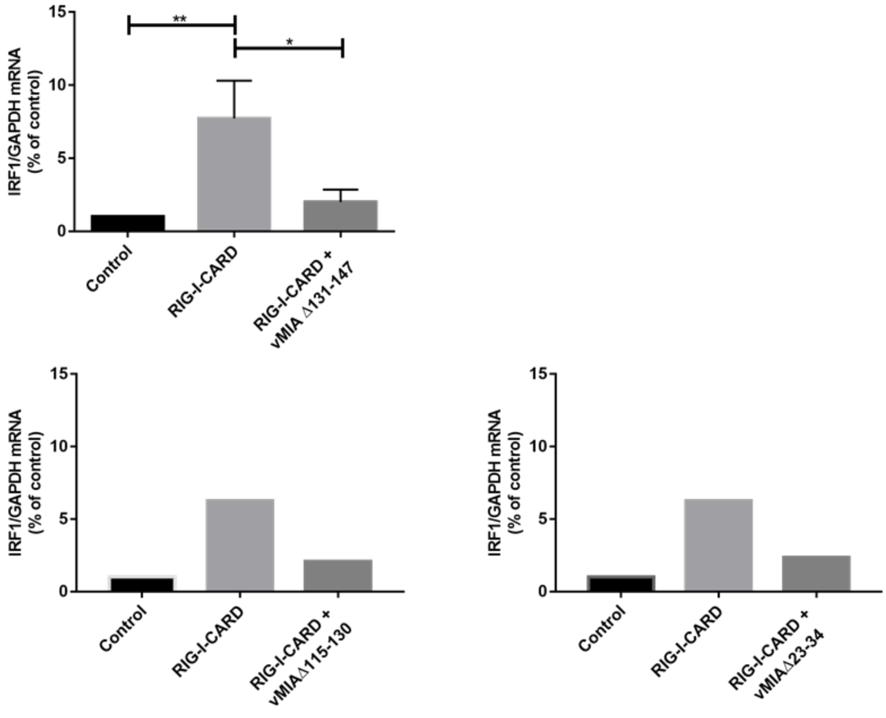

Figure 17 Deletion mutants of vMIA inhibit the peroxisome-dependent innate immunity signaling. Mefs MAVS PEX cells were transfected with deletion mutants of vMIA and stimulated with GFP-RIG-I-CARD. IRF1 mRNA expression was analyzed by RT-qPCR. GAPDH was used as a normalizer gene. For the Δ131-147, data represents the means ± SEM of three independent experiments. Statistical analysis was performed using one-way ANOVA followed by Bonferroni's multiple comparison. Error bars represent SEM. *p≤0.05, **p≤0.01, compared with control.

These results demonstrate than none of the domains that are absent in these mutants is the one responsible for the inhibition of the peroxisome-dependent antiviral response. Our results, together with what is already known in the literature, are summarized in Figure 18.

As it has been previously shown than vMIA interacts with MAVS at peroxisomes, it is highly likely that these mutants remain able to interact with this protein at the peroxisomal membrane. However, further experiments will be performed in order to confirm this interaction as well as to identify the specific domain of the protein that is responsible for the inhibition of the cellular immune response. We are currently analyzing a mutant with a deletion on the 2-23 region[41]. Whether similar results would be obtained for the mitochondria-dependent pathway remains to be investigated and will be done in the near future.

	Anti-apoptotic activity	**Bax-binding activity**	**Cellular localization**	**Organelles' fragmentation**	**Inhibition of the peroxisome-dependent antiviral response**
vMIA	+	+	Mito, ER, Golgi, PO	Mito, PO	+
Δ23-34	-	+	Cyto, ER, Mito, PO	Mito, PO	+
Δ115-130	-	-	Mito, ER, PO	none	+
Δ131-147	-	-	Mito, ER, PO	Mito, PO	+

Figure 18 Complementary characterization of vMIA and its different mutants. Obtained results with this project are underlined.

Creation of a PEX19 KO cell line

To further study the importance of the peroxisomal MAVS pathway on the antiviral immune response upon HCMV infection, we decided to create a stable cell line in which the vMIA-dependent inhibition of this pathway is compromised. It has been shown that vMIA travels to peroxisomes via interaction with Pex19[31],a 33kDa protein that acts both as a cytosolic chaperone and as an import receptor for peroxisomal membrane proteins (PMPs)[36]. It was hypothesized that, in the absence of Pex19, vMIA would not be able to reach the peroxisomal membrane, interact with MAVS and consequently inhibit the immune response.

Therefore, we decided to create a Pex19 KO cell line of human foreskin fibroblasts (HFF), a cell line that is commonly infected by HCMV, using the CRISPR/Cas9 system (Figure 19).

Lentiviral CRISPR/Cas9 constructs were generated by cloning three double-strand Pex19 oligonucleotide inserts into a puromycin resistance pSicoR-CRISPR-Cas9 (RP418) lentiviral vector. Lentiviral constructs were transfected with packaging plasmids, pCMV R8.81 and pMD2.G, into 293T cells for lentivirus production. Transduced HFF cells were expanded and further characterized by Western Blot analysis.

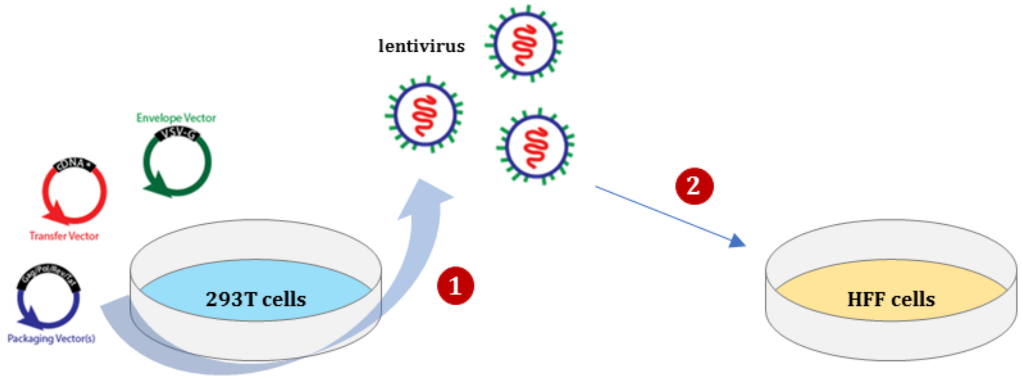

Figure 19 Schematic and shorten representation of CRISPR/Cas9 system. (1) Lentivirus production in 293T cells results from co-transfection of an envelope vestor (pMD2.G), a packaging vector (pCMV R8.81) and a pSicoR-CRISPR-Cas9 lentiviral vector (RP418) containing a PEX19 oligonucleotide insert. (2) Transduction to HFF cells and supplementary treatment with puromycin allowed KO cells selection.

The results, presented in Figure 20, suggested that the KO was effective for all oligonucleotides.

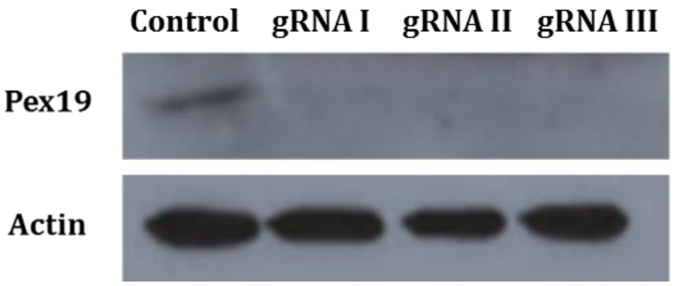

Figure 20 CRISPR/Cas9 PEX19 KO cell lines. Western blot analysis showing an effective KO of Pex19 in HFF cells. Actin was used as the loading control.

Further single cell selection is currently being performed. Once the final KO cells are obtained, these will be infected with HCMV and analyses of the intracellular vMia localization, organelle morphology, and virus production will be performed.

Study of the vMIA analogue in MCMV

HCMV replicates very slowly in cell culture and only a few cell lines (mostly HFF) are permissive to infection by this virus. Furthermore, *in vivo* infection studies with HCMV are evidently impossible. In order to overcome these drawbacks we decided to test whether we could complement our studies with the MCMV, a natural mouse pathogen that shares a high degree of sequence homology and biology with HCMV[3]. Besides being able to perform animal studies, the use of this virus would allow us to study infection in our Mefs MAVS-Pex cells as well as Mefs MAVS KO and Mefs MAVS-MITO (MAVS solely at mitochondria) cells, which are also available in the lab. Concretely, we proposed to study the m38.5

protein, which is referred as the MCMV analog to vMIA[59,60]. Although m38.5 and vMIA share little sequence similarity, their genes are located at analogous positions within the viral genomes and both share similar functions, as both localize at mitochondria where they bind Bax in order to prevent its activation and mediated apoptosis[57–59].

We decided to analyse the intracellular localization of m38.5 as well as its effect of organelle morphology and inhibition of the cellular antiviral response, in order to establish the similarity between this protein and HCMV vMia. Thus, we performed similar experiments as the previously described for the vMIA mutants. To verify the localization of m38.5, MAVS PEX cells were transfected with a HA-m38.5 construct and were subjected to immunofluorescence analysis with antibodies against the peroxisomal marker PMP70 and HA.

Analysis by confocal microscopy (Figure 21) showed an expected typical mitochondrial localization pattern as well as a co-localization with the peroxisomal marker. A preliminary analysis of the peroxisome morphology seems to indicate that, similarly to vMia, m38.5 induces the organelle's fragmentation. However, further quantification analysis will be performed in order to confirm this fact.

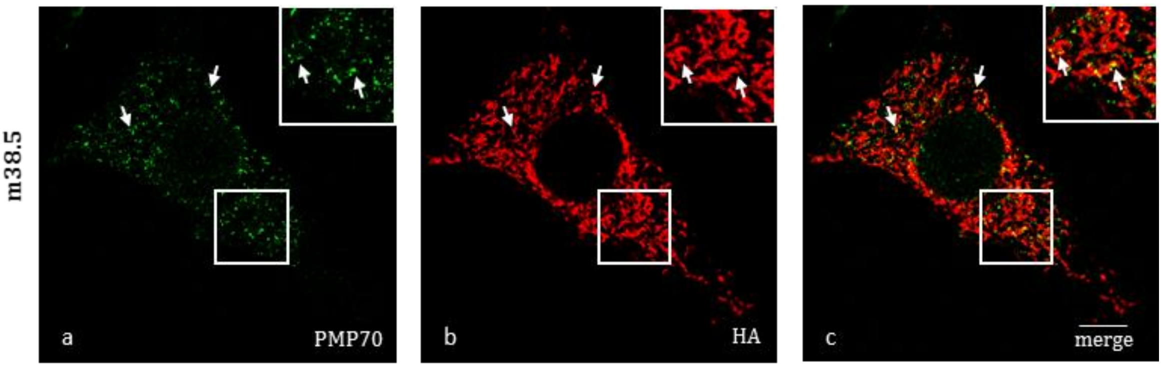

Figure 21 Peroxisomal morphology and m38.5 localization within transfected MAVS PEX cells. Confocal images of (a) PMP70, (b) Myc and (c) merge image of a and b. Bar represents 10µm. Arrows indicate co-localization loci between Myc-vMIA mutants and the peroxisomal marker.

Moreover, to examine the effect of m38.5 on the peroxisome-dependent MAVS pathway, IRF1 mRNA production was quantified by RT-qPCR. MAVS PEX cells were transfected with m38.5 for 24 hours and stimulated with GFP-RIG-I-CARD for 6 hours. The RT-qPCR results (Figure 22) indicate that, similarly to vMia, m38.5 inhibits the peroxisomal-MAVS antiviral signaling.

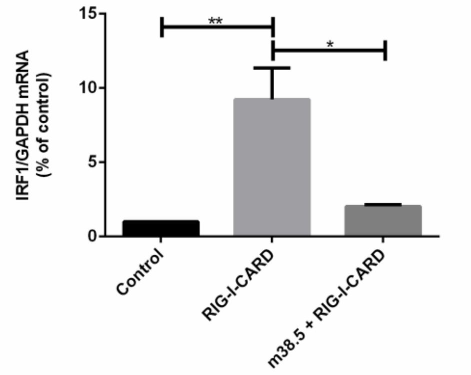

Figure 22 m38.5 inhibits MAVS PEX innate immunity signaling. Mefs MAVS PEX cells with MAVS only at peroxisomes were transfected with m38.5 and stimulated with GFP-RIG-I-CARD. Analysis of IRF1 mRNA expression by RT-qPCR showed that it is impaired by m38.5. GAPDH was used as a normalizer gene. Data represents the means ± SEM of three independent experiments. Statistical analysis was performed using one-way ANOVA followed by Bonferroni's multiple comparison. Error bars represent SEM. *$p \leq 0.05$, **$p \leq 0.01$, compared with control.

In conclusion, similarly to HCMV vMia, the MCMV m38.5 seems to localize at peroxisomes, induce the organelle's fragmentation and clearly inhibit the peroxisome-dependent antiviral immune response. Although further studies must be performed, namely on the analysis of mitochondria and mitochondria-dependent antiviral response, our results indicate that this virus may be used to complement our study with HCMV.

5.2 Influenza A Virus and Quality Control Machinery

Previous studies have shown that during viral infection specialized sites for viral replication are formed, resulting in the creation of insoluble aggregates or inclusions, which can be either part of innate cellular response[90] or used by viruses as scaffolds for replication, assembly and host immune system evasion[91]. As previously mentioned, IAV uses the aggresome processing machinery for host cell entry, specifically during uncoating[94,95].

In order to determine whether IAV infection leads to aggresomal formation, we infected HeLa cells that constitutively express a GFP-tagged HSPB1 (also named HSP27), a cellular marker form is folded proteins, and possibly aggregation (HeLa HSPB1-GFP cells). This protein is normally localized at the cytosol and relocates in foci upon stress conditions. Furthermore, the ProteoStat® Aggresome Detection Kit was used to complement our studies, as it is used to specifically detect denatured and/or misfolded protein aggregates and inclusion bodies. It contains a novel 488 nm excitable red fluorescent molecular dye to specifically detect denatured protein cargo within aggresomes and aggresome-like inclusion bodies in fixed and permeabilized cells.

HeLa HSPB1-GFP cells were infected with PR8 and ΔNS1 viruses and fixed cells for immunofluorescence analysis were collected 1 hour post infection (hpi), 2hpi, 4hpi, 8hpi, 12hpi and 16hpi. PR8 stands for the wild-type of influenza strain A/Puerto Rico/8/1934 (H1N1), while ΔNS1 stands for a NS1-deleted mutant from the same strain. The NS1 protein is a non-essential virulence factor that has been described as essential for inhibition of host immune responses, especially through the limitation of IFN production[118,119]. Thus, the ΔNS1 virus mutant is less capable of subvert antiviral cellular response and we expected a slower life cycle, comparing to PR8 virus.

After overcoming some technical constrains on the establishment of the IAV infection procedure in our laboratory, we were able to perform a preliminary analysis by confocal microscopy which indicated the formation of aggregates/aggresomes in ΔNS1 infected cells (Figure 23) at a time-point where the vRNP are not yet present in the nucleus. These aggregates tend to disappear in later time points (data not shown). This preliminary analysis did not show the presence of protein aggregates in PR8-infected cells.

It was previously shown by that Banerjee et al[95] that IAV takes advantage of the aggresome processing machinery for host cell entry, using immunoprecipitation and immune colocalization assays between viral and aggresome machinery-associated proteins. They demonstrated that IAV requires the ubiquitin-binding function of HDAC6 for capsid uncoating and viral content release into the cytosol, including M1 protein and the vRNPs that are further transported to the nucleus (Figure 10). Besides HDAC6, other key components of the aggresome processing machinery, namely dynein, dynactin, and myosin II, proved to be also required for an efficient infection[95].

Therefore, our results are somewhat consistent with these, since we observe aggresome formation before nuclear vRNP staining. Taking Banerjee et al[95] results in consideration, we hypothesize that these aggregates may correspond to sites of uncoating and vRNP release. In future studies, we propose to characterize the originated aggresomes in terms of protein content.

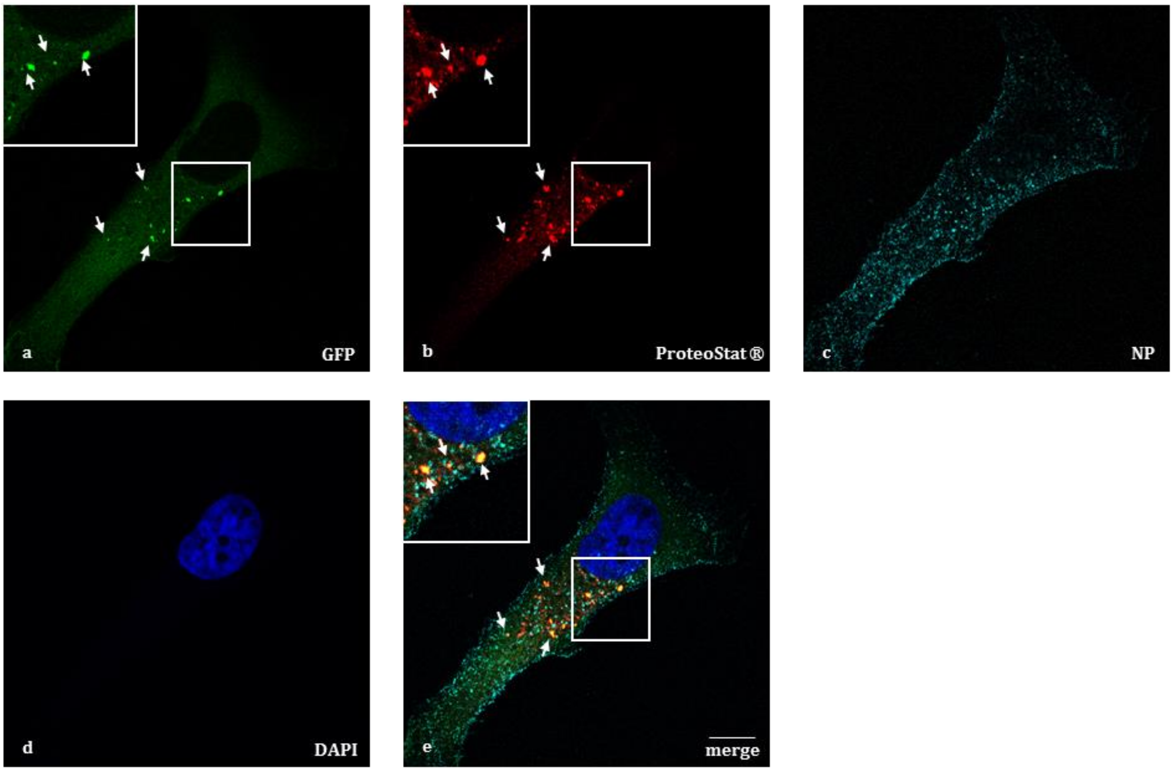

Figure 23 Aggresomal formation in HeLa HSPB1-GFP cells infected with ΔNS1 IAV. Confocal images of (a) cellular HSPB1-GFP, (b) Proteostat dye, (c) viral NP, (d) nuclear DAPI, and (e) merge image. Bar represents 10μm. Arrows indicate protein aggregates.

Simultaneously, we have analyzed the insoluble protein fraction within the cells throughout the infection-course. To conduct the experiment, HeLa HSPB1-GFP cells were infected with PR8 and ΔNS1, total protein was extracted using ELB supplemented with protease inhibitors, from which a detergent-insoluble fraction was obtained. Protein samples ran by SDS-PAGE, were stained with BlueSafe, and quantified (Figure 24). Our preliminary results indicate an increase in the insoluble protein fraction upon IAV infection, mainly with the ΔNS1 virus. These results suggest that there may occur an accumulation of misfolded aggregation-prone proteins upon IAV infection. However, more replicated need to be performed in or to take a more solid conclusion.

It is known that viral infection can lead to accumulation of unfolded proteins and its aggregation within the ER, inducing ER stress and consequently the UPR[97]. Thus, we proposed to analyze UPR induction through ATF6 activation. In cells undergoing ER stress, ATF6 (75 kDa) is cleaved into an active cytosolic fragment (ATF6f, 50 kDa) that activates the molecular chaperone transcription to increase ER folding capacity.

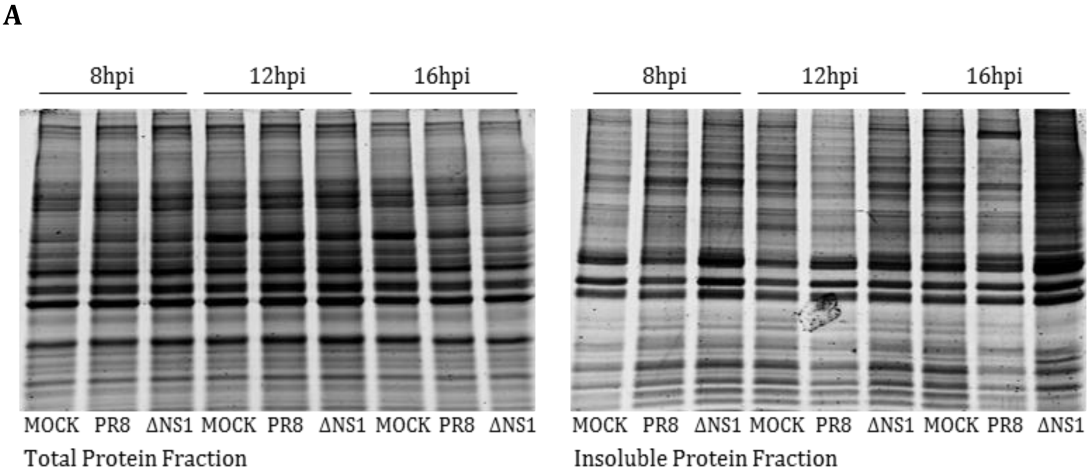

B **Insoluble/Total Ratio**

	8hpi	**12hpi**	**16hpi**
mock	1.000	1.000	1.000
PR8	1.529	1.071	0.957
ΔNS1	1.542	1.171	1.364

Figure 24 Caracterization of insoluble protein fraction upon infection at different time points, normalized to the total fraction. (A) SDS PAGE of total and insoluble protein fraction of infection with both different viruses, at 8, 12 and 16hpi. (B) Dermination of the insoluble/total ration of each condition in relation to mock cells.

To our knowledge, the previous results on this study are somehow contradictory. Hassan et al.[113] reported that IAV modulates the stress response in the setting of a pre-existing stress, by decreasing the activation of the ATF6 pathway; Roberson et al.[114] showed, in murine cells, that IAV infection induces ER-stress via ATF6 activation; and Landeras-Bueno et al.[115] found that IAV does not downregulate ATF6.

In our study, the cleavage of ATF6 into ATF6f in human cells was analyzed by immunoblotting. HeLa HSPB1-GFP cells were infected and proteins were extracted as previously described. The obtained results suggest an increment of ATF6 cleavage with time upon PR8 and ΔNS1virus infection (Figure 25).

These results, although preliminary, corroborate those from Roberson et al[114] that presented in MTEC cells an increase in ATF6 by Western blotting at 24hpi, which was sustained up to 48hpi, using a mouse-adapted IAV PR/8/34 (H1N1).

However, our results are inconsistent with Hassan et al[113] that showed no activation of ATF6 upon infection, but an inhibition of a preexisting induced ER stress. In this case, the authors also studied IAV PR/8/34 (H1N1) influence on ATF6 pathway at similar times of infection, explicitly 12hpi, however with a different approach. They rely on HTBE cells infected with a multiplicity of infection (MOI) of 1, and measured the ATF6 inhibition using q-RT-PCR of some ATF6-driven stress genes. In this study, we followed a different approach by trying to characterize, in a different cell line, the ATF6 pathway activation by directly detecting and measuring its cleavage. This is not impeditive that these genes are inhibited downstream ATF6 cleavage, for instance as a consequence of crosstalk with other responses happening concomitantly within the cell.

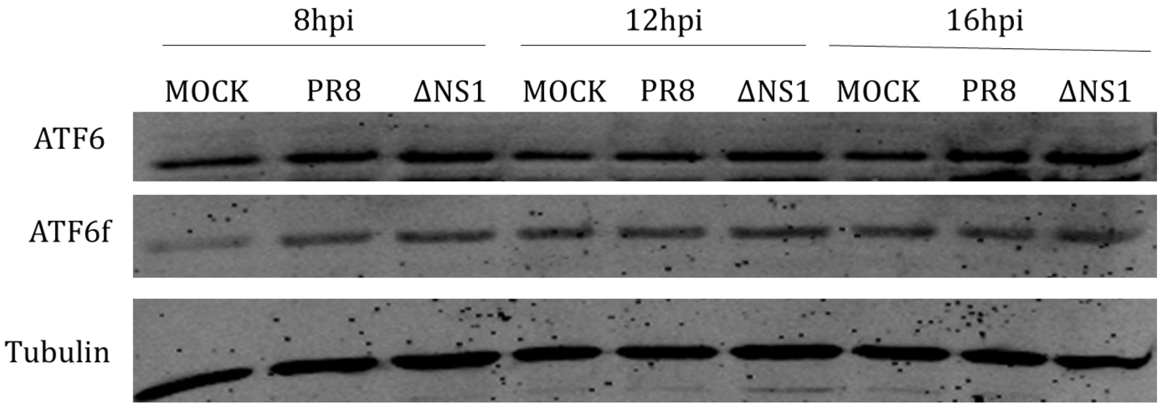

B

	ATF6f/tubulin ratio		
	8hpi	**12hpi**	**16hpi**
mock	1	1	1
PR8	2.59	1.12	1.68
ΔNS1	3.19	2.11	3.23

Figure 25 ATF6 is activated upon IAV infection. (A) Protein extracted from HeLa HSPB1-GFP cells infected with both PR8 and ΔNS1 viruses for 8, 12 and 16 hpi, were analyzed by immunoblotting for ATF6 fragmentation. Tubulin was used as loading control. (B) Determination of ATF6f/tubulin ratio in relation to mock cells.

In parallel, we are currently optimizing the antibodies for PERK, IRE1 and their phosphorylated forms, in order to further analyze the PERK and IRE1 pathways.

CONCLUDING REMARKS

Human Cytomegalovirus and Innate Immunity

HCMV vMIA has been shown to localize at mitochondria and peroxisomes, induce their fragmentation and, more importantly, inhibit the cellular antiviral response that is established at these organelles. With the objective of unraveling the mechanisms by which vMia is able to exert these changes, we decided to study several mutants of these proteins that lack specific aminoacid sequences. In this way, we were able to conclude that the 115-130 amino acid sequence is likely the domain responsible for peroxisomes and mitochondria fragmentation. However, none of the studied mutants was incapable of inhibiting the peroxisome-dependent immune response. We are currently testing other mutants and performing further analysis in order to confirm and expand our results. We have also initiated the creation of a HFF Pex19 KO cell line using CRISPR/Cas9. As vMia is not able to reach the peroxisomes without the help of Pex19, once this cell line is fully prepared, we will be able to infect it with HCMV and analyse whether (and where in the virus life-cycle) the peroxisome-dependent antiviral pathway is important for inhibiting viral proliferation. Moreover, we have demonstrated that the MCMV m38.5 seems to act similarly to vMIA, in what organelle's morphology changes and inhibition of the peroxisomal antiviral response are concerned. We are now, hence, able to use this virus to complement our results on HCMV and able to, in the future, replicate our experiments in infected animal models.

Influenza A Virus and Quality Control Machinery

During infection, the formation of specialized sites of viral replication can result in the formation of insoluble aggregates or inclusions that may be part of innate cellular response that recognizes and sequesters viral components, or possibly will be used by viruses as scaffolds for anchoring either viral and host proteins required for replication and assembly, as a protection from host defense. It is known that IAV requires HDAC6 ubiquitin-binding function, taking advantage of the aggresome processing machinery for host cell entry and especially for capsid uncoating. Also, during productive viral infection, as in the case of IAV, large amounts of viral proteins are synthesized and modified in infected cells, leading to rapid accumulation of viral proteins and disruption of the ER homeostasis and induction of UPR. Our results, although preliminary, indicate that there is formation of aggresomes upon infection, as well as an accumulation of insoluble proteins in IAV-infected cells. Naturally, these results must be complemented with further replicates and, if confirmed, we will characterize aggresome dynamics and composition over the course of infection. Our results also indicate that the UPR ATF6 pathway is influenced by IAV infection. These results have to be confirmed with more replicates and the behavior of the other two UPR pathways upon IAV infection will also be studied in the near future.

Publications resulting from this work

Gouveia A., Ferreira A.R., Magalhães, A.C., Marques M., Sampaio P., Schrader M. and Ribeiro D. "Cytomegalovirus evasion from the RIG-I/MAVS-dependent antiviral response follows discting mechanisms in peroxisomes and mitochondria.", manuscript in preparation.

REFERENCES

1. Baltimore D. Expression of animal virus genomes. *Bacteriol Rev*. 1971;35(3):235-241.
2. Shenk T, Alwine JC. Human Cytomegalovirus: Coordinating Cellular Stress, Signaling, and Metabolic Pathways. *Annu Rev Virol*. 2014;1(1):355-374. doi:10.1146/annurev-virology-031413-085425.
3. Brune W, Andoniou C. Die Another Day: Inhibition of Cell Death Pathways by Cytomegalovirus. *Viruses*. 2017;9(9):249. doi:10.3390/v9090249.
4. Cannon MJ, Schmid DS, Hyde TB. Review of cytomegalovirus seroprevalence and demographic characteristics associated with infection. *Rev Med Virol*. 2010;20(4):202-213.
5. Sia IG, Patel R. New strategies for prevention and therapy of cytomegalovirus infection and disease in solid-organ transplant recipients. *Clin Microbiol Rev*. 2000;13:83-121.
6. Ho M. The history of cytomegalovirus and its diseases. *Med Microbiol Immunol*. 2008;197(2):65-73.
7. Dupont L, Reeves MB. Cytomegalovirus latency and reactivation: recent insights into an age old problem. *Rev Med Virol*. 2016;26(2):75-89. doi:10.1002/rmv.1862.
8. Mocarski ES, Shenk T, Pass RF. *Fields Virology*. (Knipe, D. M. & Howley PM, ed.). Lippincott Williams & Wilkins; 2007.
9. Ahmed A. Antiviral treatment of cytomegalovirus infection. *Infect Disord Drug Targets*. 2011;11(5):475-503. http://www.ncbi.nlm.nih.gov/pubmed/21827432.
10. Kalejta RF. Tegument Proteins of Human Cytomegalovirus. *Microbiol Mol Biol Rev*. 2008;72(7):249-265.
11. Bresnahan W, Shenk T. A Subset of Viral Transcripts Packaged Within Human Cytomegalovirus Particles. *Science (80-)*. 2000;288(5475):2373-2376.
12. Wille PT, Wisner TW, Ryckman B, Johnson DC. Human cytomegalovirus (HCMV) glycoprotein gB promotes virus entry in Trans acting as the viral fusion protein rather than as a receptor-binding protein. *MBio*. 2013;4(3):1-9. doi:10.1128/mBio.00332-13.
13. Beltran PMJ, Cristea IM. The lifecycle and pathogenesis of human cytomegalovirus infection: lessons from proteomics. *Expert Rev Proteomics*. 2015;11(6):697-711. doi:10.1586/14789450.2014.971116.The.
14. Sissons JG, Bain M, Wills MR. Latency and reactivation of human cytomegalovirus. *J Infect*. 2002;44:78-83.
15. Jarvis MA, Nelson JA. Mechanisms of human cytomegalovirus persistence and latency. *Front Biosci*. 2002;7:d1575-1582.
16. Crough T, Khanna R. Immunobiology of Human Cytomegalovirus: from Bench to Bedside. *Clin*

Microbiol Rev. 2009;22(1):76-98. doi:10.1128/CMR.00034-08.

17. Valentine H, Luikart H, Doyle R, Theodore J, Hunt S, Oyer P. Impact of Cytomegalovirus hyperimmune globulin on outcome after cardiothoracic transplantation: a comparative study of combined pprophylaxis with CMV hyperimmune globulin plus ganciclovir versus ganciclovir alone. *Transplantation*. 2001;72(10):1647-1652.

18. Liu Y, Olagnier D, Lin R. Host and viral modulation of RIG-I-mediated antiviral immunity. *Front Immunol*. 2017;7(JAN):1-12. doi:10.3389/fimmu.2016.00662.

19. Kumar H, Kawai T, Akira S. Pathogen Recognition by the Innate Immune System. *Int Rev Immunol*. 2011;30(1):16-34. doi:10.3109/08830185.2010.529976.

20. Odendall C, Kagan JC. Peroxisomes and their Key Role in Cellular Signaling and Metabolism. *Subcell Biochem*. 2013;69:67-75. doi:10.1007/978-94-007-6889-5.

21. West JA, Gregory SM, Damania B. Toll-like receptor sensing of human herpesvirus infection. *Front Cell Infect Microbiol*. 2012.

22. Yew KH, Carpenter C, Duncan RS, Harrison CJ. Human Cytomegalovirus Induces TLR4 Signaling Components in Monocytes Altering TIRAP, TRAM and Downstream Interferon-Beta and TNF-Alpha Expression. *PLoS One*. 2012;7(9):1-17. doi:10.1371/journal.pone.0044500.

23. Tabeta K, Georgel P, Janssen E, et al. Toll-like receptors 9 and 3 as essential components of innate immune defense against mouse cytomegalovirus infection. *Proc Natl Acad Sci U S A*. 2004;101(10):3516-3521. doi:10.1073/pnas.0400525101.

24. Kim JE, Kim YE, Stinski MF, Ahn JH, Song YJ. Human cytomegalovirus IE2 86 kDa protein induces STING degradation and inhibits cGAMP-mediated IFN-β induction. *Front Microbiol*. 2017;8(SEP):1-14. doi:10.3389/fmicb.2017.01854.

25. Fu Y, Su S, Gao Y, et al. Human Cytomegalovirus Tegument Protein UL82 Inhibits STING-Mediated Signaling to Evade Antiviral Immunity. *Cell Host Microbe*. 2017;21(2):231-243.

26. Lio C-WJ, McDonald B, Takahashi M, et al. cGAS-STING Signaling Regulates Initial Innate Control of Cytomegalovirus Infection. *J Virol*. 2016;90(17):7789-7797. doi:10.1128/JVI.01040-16.

27. Yoneyama M, Kikuchi M, Matsumoto K, et al. Shared and unique functions of the DExD/H-box helicases RIG-I, MDA5, and LGP2 in antiviral innate immunity. *J Immunol*. 2005;175:2851-2858.

28. Onomoto K, Yoneyama M, Fung G, Kato H, Fujita T. Antiviral innate immunity and stress granule responses. *Trends Immunol*. 2014;35(9):420-428. doi:10.1016/j.it.2014.07.006.

29. Belgnaoui SM, Paz S, Hiscott J. Orchestrating the interferon antiviral response through the mitochondrial antiviral signaling (MAVS) adapter. *Curr Opin Immunol*. 2011;23(5):564-572. doi:10.1016/j.coi.2011.08.001.

30. Biacchesi S, Me E, Lamoureux A, Bernard J, Bre M. Both STING and MAVS Fish Orthologs Contribute to the Induction of Interferon Mediated by RIG-I. *PLoS One*. 2012;7(e477737).

31. Magalhães AC, Ferreira AR, Gomes S, et al. Peroxisomes are platforms for cytomegalovirus' evasion from the cellular immune response. *Sci Rep*. 2016;6(1):26028. doi:10.1038/srep26028.

32. Horner SM, Liu HM, Park HS, Briley J, Gale M. Mitochondrial-associated endoplasmic reticulum membranes (MAM) form innate immune synapses and are targeted by hepatitis C virus. *Proc Natl Acad Sci*. 2011;108(35):14590-14595. doi:10.1073/pnas.1110133108.

33. Dixit E, Boulant S, Zhang Y, et al. Peroxisomes Are Signaling Platforms for Antiviral Innate Immunity. *Cell*. 2010;141(4):668-681. doi:10.1016/j.cell.2010.04.018.

34. Camões F, Bonekamp NA, Delille HK, Schrader M. Organelle dynamics and dysfunction: A closer link between peroxisomes and mitochondria. *J Inherit Metab Dis*. 2009;32(2):163-180. doi:10.1007/s10545-008-1018-3.

35. Fransen M, Lismont C, Walton P. The peroxisome-mitochondria connection: How and why? *Int J Mol Sci*. 2017;18(6). doi:10.3390/ijms18061126.

36. Islinger M, Grille S, Fahimi HD, Schrader M. The peroxisome: an update on mysteries. *Histochem Cell Biol*. 2012;137(5):547-574.

37. Lodhi IJ, Semenkovich FC. Peroxisomes: A Nexus for Lipid Metabolism and Cellular Signaling. *Cell Metab Elsevier Inc*. 2014;19(3):380-392.

38. Hou F, Sun L, Zheng H, Skaug B, Jiang Q-X, Chen ZJ. MAVS Forms Functional Prion-Like Aggregates To Activate and Propagate Antiviral Innate Immune Response. *Cell*. 2011;146(3):448-461. doi:10.1016/j.cell.2011.06.041.MAVS.

39. Sharma S, Fitzgerald KA. Viral Defense: It Takes Two MAVS to Tango. *Cell*. 2010;141(4):570-572. doi:10.1016/j.cell.2010.04.043.

40. Elmore S. A Review of Programmed Cell Death. *Toxicol Pathol*. 2007;35(4):495-516.

41. Goldmacher VS, Bartle LM, Skaletskaya A, et al. A cytomegalovirus-encoded mitochondria-localized inhibitor of apoptosis structurally unrelated to Bcl-2. *Proc Natl Acad Sci U S A*. 1999;96(22):12536-12541. doi:10.1073/PNAS.96.22.12536.

42. McCormick AL, Meiering CD, Smith GB, Mocarski ES. Mitochondrial cell death suppressors carried by human and murine cytomegalovirus confer resistance to proteasome inhibitor-induced apoptosis. *J Virol*. 2005;79(19):12205-12217. doi:10.1128/JVI.79.19.12205-12217.2005.

43. Sharon-Friling R, Goodhouse J, Colberg-Poley AM, Shenk T. Human cytomegalovirus pUL37x1 induces the release of endoplasmic reticulum calcium stores. *Proc Natl Acad Sci U S A*.

2006;103:19117-19122. doi:10.1073/pnas.0609353103.

44. Hayajneh WA, Colberg-Poley AM, Skaletskaya A, et al. The sequence and antiapoptotic functional domains of the human cytomegalovirus UL37 exon 1 immediate early protein are conserved in multiple primary strains. *Virology*. 2001;279:233-240.

45. Mavinakere MS, Colberg-Poley AM. Dual targeting of the human cytomegalovirus UL37 exon 1 protein during permissive infection. *J Gen Virol*. 2004;85(2):323-329. doi:10.1099/vir.0.19589-0.

46. Arnoult D, Bartle LM, Skaletskaya A, et al. Cytomegalovirus cell death suppressor vMIA blocks Bax- but not Bak-mediated apoptosis by binding and sequestering Bax at mitochondria. *Proc Natl Acad Sci U S A*. 2004;101:7988-7993.

47. Pauleau AL, Larochette N, Giordanetto F, et al. Structure-function analysis of the interaction between Bax and the cytomegalovirus-encoded protein vMIA. *Oncogene*. 2007;26(50):7067-7080. doi:10.1038/sj.onc.1210511.

48. Kaarbø M, Ager-Wick E, Osenbroch P, et al. Human cytomegalovirus infection increases mitochondrial biogenesis. *Mitochondrion*. 2011;11(6):935-945.

49. Schrader M, Bonekamp N, Islinger M. Fission and proliferation of peroxisomes. *Biochim Biophys Acta Elsevier BV*. 2012;1822(9):1343-1357.

50. Rucktäschel R, Halbach A, Girzalsky W, Rottensteiner H, Erdmann R. De novo synthesis of peroxisomes upon mitochondrial targeting of Pex3p. *Eur J Cell Biol*. 2010;89(12):947-954.

51. Schrader M. Shared components of mitochondrial and peroxisomal division. *Biochim Biophys Acta - Mol Cell Res*. 2006;1763(5-6):531-541. doi:10.1016/j.bbamcr.2006.01.004.

52. Schrader M, Costello JL, Godinho LF, Azadi AS, Islinger M. Proliferation and fission of peroxisomes - An update. *Biochim Biophys Acta - Mol Cell Res*. 2016;1863(5):971-983. doi:10.1016/j.bbamcr.2015.09.024.

53. McCormick AL, Smith VL, Chow D, Mocarski ES. Disruption of Mitochondrial Networks by the Human Cytomegalovirus UL37 Gene Product Viral Mitochondrion-Localized Inhibitor of Apoptosis. *J- Virol*. 2003;77:631-641.

54. Castanier C, Garcin D, Vazquez A, Arnoult D. Mitochondrial dynamics regulate the RIG-I-like receptor antiviral pathway. *EMBO Rep*. 2010;11(2):133-138. doi:10.1038/embor.2009.258.

55. Goldmacher VS. vMIA, a viral inhibitor of apoptosis targeting mitochondria. *Biochimie*. 2002;84:177-185.

56. Fliss PM, Brune W. Prevention of cellular suicide by cytomegaloviruses. *Viruses*. 2012;4(10):1928-1949. doi:10.3390/v4101928.

57. Norris KL, Youle RJ. Cytomegalovirus proteins vMIA and m38.5 link mitochondrial morphogenesis to Bcl-2 family proteins. *J Virol*. 2008;82(13):6232-6243. doi:10.1128/JVI.02710-07.

58. Cam M, Handke W, Picard-Maureau M, Brune W. Cytomegaloviruses inhibit Bak- and Bax-mediated apoptosis with two separate viral proteins. *Cell Death Differ*. 2010;17(4):655-665. doi:10.1038/cdd.2009.147.

59. Jurak I, Schumacher U, Simic H, Voigt S, Brune W. Murine cytomegalovirus m38.5 protein inhibits Bax-mediated cell death. *J Virol*. 2008;82(10):4812-4822.

60. Handke W, Krause E, Brune W. Live or let die: Manipulation of cellular suicide programs by murine cytomegalovirus. *Med Microbiol Immunol*. 2012;201(4):475-486. doi:10.1007/s00430-012-0264-z.

61. Taubenberger JK, Morens DM. The Pathology of Influenza Virus Infections. *Annu Rev Pathol*. 2008;3(1):499-522. doi:10.1038/nrm2621.

62. Noda T. Native morphology of influenza virions. *Front Microbiol*. 2012;2(JAN):1-5. doi:10.3389/fmicb.2011.00269.

63. Das K, Aramini JM, Ma L-C, Krug RM, Arnold E. Structures of influenza A proteins and insights into antiviral drug targets. *Nat Struct Mol Biol*. 2010;17(5):530-538. doi:10.1038/nsmb.1779.

64. Samji T. Influenza A: Understanding the viral life cycle. *Yale J Biol Med*. 2009;82(4):153-159.

65. Torres-González E, Bueno M, Tanaka A, et al. Role of endoplasmic reticulum stress in age-related susceptibility to lung fibrosis. *Am J Respir Cell Mol Biol*. 2012;46(6):748-756. doi:10.1165/rcmb.2011-0224OC.

66. Guilligay D, Tarendeau F, Resa-Infante P, et al. The structural basis for cap binding by influenza virus polymerase subunit PB2. *Nat Struct Mol Biol*. 2008;15:500-506.

67. Dias A, Bouvier D, Crépin T, et al. The cap-snatching endonuclease of influenza virus polymerase resides in the PA subunit. *Nature*. 2009;458(7240):914-918. doi:10.1038/nature07745.

68. Marreiros R, M??ller-Schiffmann A, Bader V, et al. Viral capsid assembly as a model for protein aggregation diseases: Active processes catalyzed by cellular assembly machines comprising novel drug targets. *Virus Res*. 2015;207:155-164. doi:10.1016/j.virusres.2014.10.003.

69. Reich S, Guilligay D, Pflug A, et al. Structural insight into cap-snatching and RNA synthesis by influenza polymerase. *Nature*. 2014;516(7531):361-366. doi:10.1038/nature14009.

70. Briedis DJ. *Influenza Viruses. Fundamentals of Molecular Virology*. 2nd ed. Wiley; 2011.

71. McNicholl IR, McNicholl JJ. Neuraminidase inhibitors: zanamivir and oseltamivir. *Ann Pharmacother*. 2001;35(1):57-50.

72. Min J-Y, Subbarao K. Cellular targets for influenza drugs: High-throughput RNAi screens in human cells suggest new approaches to curb influenza virus infection. *Nat Biotechnol*. 2010;28(3):230-240. doi:10.1086/498510.Parasitic.

73. Rajan RS, Illing ME, Bence NF, Kopito RR. Specificity in intracellular protein aggregation and inclusion body formation. *Proc Natl Acad Sci*. 2001;98:13060–13065.

74. Dobson CM. Protein folding and misfolding. *Nature*. 2003;426:884-890.

75. Stefani M. Protein misfolding and aggregation: New examples in medicine and biology of the dark side of the protein world. *Biochim Biophys Acta - Mol Basis Dis*. 2004;1739(1):5-25. doi:10.1016/j.bbadis.2004.08.004.

76. Marquardt T, Helenius A. Misfolding and aggregation of newly synthesized proteins in the endoplasmic reticulum. *J Cell Biol*. 1992;117(3):505-513. doi:10.1083/jcb.117.3.505.

77. Johnston JA, Ward CL, Kopito RR. A Cellular Response to Misfolded Proteins Aggresomes : *Cell*. 2012;143(7):1883-1898. doi:10.1083/jcb.143.7.1883.

78. Tyedmers J, Mogk A, Bukau B. Cellular strategies for controlling protein aggregation. *Nat Rev Mol Cell Biol*. 2010;11(11):777-788. doi:10.1038/nrm2993.

79. Feldman DE, Frydman J. Protein folding in vivo: the importance of molecular chaperones. *Curr Opin Struct Biol*. 2000;10(1):26-33.

80. Chakrabarti A, Chen AW, Varner JD. A Review of the Mammalian Unfolded Protein Response. *Biotechnol Bioeng*. 2011;108(12):2777-2793. doi:10.1002/bit.23282.A.

81. Lamark T, Johansen T. Aggrephagy: Selective disposal of protein aggregates by macroautophagy. *Int J Cell Biol*. 2012;2012. doi:10.1155/2012/736905.

82. Su H, Wang X. The ubiquitin-proteasome system in cardiac proteinopathy: A quality control perspective. *Cardiovasc Res*. 2010;85(2):253-262. doi:10.1093/cvr/cvp287.

83. Jovaisaite V, Mouchiroud L, Auwerx J. The mitochondrial unfolded protein response , a conserved stress response pathway with implications in health and disease. 2014:137-143. doi:10.1242/jeb.090738.

84. Li J, Chai Q-Y, Liu CH. The ubiquitin system: a critical regulator of innate immunity and pathogen–host interactions. *Cell Mol Immunol*. 2016;13(5):560-576. doi:10.1038/cmi.2016.40.

85. Fung TS, Torres J, Liu DX. The Emerging Roles of Viroporins in ER Stress Response and Autophagy Induction during Virus Infection. 2015;2:2834-2857. doi:10.3390/v7062749.

86. Garcia-Mata R, Gao Y-S, Sztul E. Hassles with taking out the garbage: aggravating aggresomes. *Traffic*. 2002;3(6):388-396. doi:tra030602 [pii].

87. Purves D, Augustine GJ, Fitzpatrick D, et al. *Neuroscience.* Third Edit. (Sinauer Associates I, ed.).

Sunderland, Massachusetts; 2004.

88. Mathias Jucker LCW. Self-propagation of pathogenic aggregates in neurodegenerative diseases. *Nature*. 2013;501(7465):45-51. doi:10.1038/nature12481.Self-propagation.

89. Li ZF, Wu X, Jiang Y, et al. Non-pathogenic protein aggregates in skeletal muscle in MLF1 transgenic mice. *J Neurol Sci*. 2008;264(1-2):77-86. doi:10.1016/j.jns.2007.07.027.

90. Moshe A, Gorovits R. Virus-Induced Aggregates in Infected Cells. *Viruses*. 2012;4:2218-2232. doi:10.3390/v4102218.

91. Wileman T. Aggresomes and Pericentriolar Sites of Virus Assembly: Cellular Defense or Viral Design? *Annu Rev Microbiol*. 2007;61(1):149-167. doi:10.1146/annurev.micro.57.030502.090836.

92. Kopito RR. Aggresomes, inclusion bodies and protein aggregation. *Trends Cell Biol*. 2000;10(12):524-530. doi:10.1016/S0962-8924(00)01852-3.

93. Kawaguchi Y, Kovacs JJ, McLaurin A, Vance JM, Ito A, Yao TP. The deacetylase HDAC6 regulates aggresome formation and cell viability in response to misfolded protein stress. *Cell*. 2003;115(6):727-738. doi:10.1016/S0092-8674(03)00939-5.

94. Rudnicka A, Yamauchi Y. Ubiquitin in influenza virus entry and innate immunity. *Viruses*. 2016;8(10):1-15. doi:10.3390/v8100293.

95. Banerjee I, Miyake Y, Nobs SP, Matthias P, Helenius A, Yamauchi Y. Influenza Avirus uses the aggresome processing machinery for host cell entry. *Science (80-)*. 2013;14167(2001):14162-14167.

96. Schr M, Kaufman RJ. ER stress and the unfolded protein response. 2005;569:29-63. doi:10.1016/j.mrfmmm.2004.06.056.

97. Verchot J. ScienceDirect How does the stressed out ER find relief during virus infection ? *Curr Opin Virol*. 2016;17:74-79. doi:10.1016/j.coviro.2016.01.018.

98. Kapoor A, Sanyal AJ. Endoplasmic Reticulum Stress a nd the Unfolde d Protein Resp ons e. *Clin Liver Dis*. 2009;13(4):581-590. doi:10.1016/j.cld.2009.07.004.

99. Maurel M, Chevet E, Tavernier J, Gerlo S. Getting RIDD of RNA : IRE1 in cell fate regulation. *Trends Biochem Sci*. 2014:1-10. doi:10.1016/j.tibs.2014.02.008.

100. Coelho DS, Domingos PM. Physiological roles of regulated Ire1 dependent decay. 2014;5(April):1-6. doi:10.3389/fgene.2014.00076.

101. Ogen-shtern N, Ben T, Lederkremer GZ. Protein aggregation and ER stress. *Brain Res*. 2016:1-9. doi:10.1016/j.brainres.2016.03.044.

102. Iurlaro R. Cell death induced by endoplasmic reticulum stress. 2015:1-13.

doi:10.1111/febs.13598.

103. Hetz C. The unfolded protein response : controlling cell fate decisions under ER stress and beyond. *Nat Publ Gr*. 2012;13(2):89-102. doi:10.1038/nrm3270.

104. Walter P, Ron D. The Unfolded Protein Response : 2012;1081(2011). doi:10.1126/science.1209038.

105. Zhang L, Wang A. Virus-induced ER stress and the unfolded protein response. 2012;3(December):1-16. doi:10.3389/fpls.2012.00293.

106. Kourtis N, Tavernarakis N. EMBO Member ' s Review Cellular stress response pathways and ageing : intricate molecular relationships. *EMBO J*. 2011;30(13):2520-2531. doi:10.1038/emboj.2011.162.

107. Li S, Kong L, Yu X. The expanding roles of endoplasmic reticulum stress in virus replication and pathogenesis. 2013;7828:1-15. doi:10.3109/1040841X.2013.813899.

108. Horng J. ER stress , autophagy , and RNA viruses. *Front Microbiol*. 2014;5:1-13. doi:10.3389/fmicb.2014.00388.

109. Smith JA. A new paradigm : innate immune sensing of viruses via the unfolded protein response. *Front Microbiol*. 2014;5:1-10. doi:10.3389/fmicb.2014.00222.

110. Samarasinghe AE, You D, Cormier SA. Acute Lung Injury Results from Innate Sensing of Viruses by an. *Cell Rep*. 2015;11(10):1591-1603. doi:10.1016/j.celrep.2015.05.012.Acute.

111. Chan S. The unfolded protein response in virus infections. 2014;5(September):1-2. doi:10.3389/fmicb.2014.00518.

112. Goodman AG, Smith JA, Balachandran S, et al. The cellular protein P58IPK regulates influenza virus mRNA translation and replication through a PKR-mediated mechanism. *J Virol*. 2007;81(5):2221-2230. doi:10.1128/JVI.02151-06.

113. Hassan IH, Zhang MS, Powers LS, et al. Influenza A viral replication is blocked by inhibition of the inositol-requiring enzyme 1 (IRE1) stress pathway. *J Biol Chem*. 2012;287(7):4679-4689. doi:10.1074/jbc.M111.284695.

114. Roberson EC, Tully JE, Guala AS, et al. Influenza induces endoplasmic reticulum stress, caspase-12-dependent apoptosis, and c-Jun N-terminal kinase-mediated transforming growth factor-β release in lung epithelial cells. *Am J Respir Cell Mol Biol*. 2012;46(5):573-581. doi:10.1165/rcmb.2010-0460OC.

115. Landeras-bueno S, Fernández Y, Falcón A, Oliveros C. Chemical Genomics Identifies the PERK-Mediated Unfolded Protein. *MBio*. 2016;7(2):1-13. doi:10.1128/mBio.00085-16.Invited.

116. Poncet D, Larochette N, Pauleau AL, et al. An antiapoptotic viral protein that recruits Bax to

mitochondria. *J Biol Chem*. 2004;279:22605-22614.

117. Ferreira AR, Magalhães AC, Camões F, et al. Hepatitis C virus NS3-4A inhibits the peroxisomal MAVS-dependent antiviral signalling response. *J Cell Mol Med*. 2016;20(4):750-757. doi:10.1111/jcmm.12801.

118. García-Sastre A, Egorov A, Matassov D, et al. Influenza A Virus Lacking the NS1 Gene Replicates in Interferon-Deficient Systems. *Virology*. 1998;252(2):324-330. doi:10.1006/viro.1998.9508.

119. Guo Z, Chen LM, Zeng H, et al. NS1 protein of influenza A virus inhibits the function of intracytoplasmic pathogen sensor, RIG-I. *Am J Respir Cell Mol Biol*. 2007;36(3):263-269. doi:10.1165/rcmb.2006-0283RC.